NASA/TM–2002–206892, Vol. 21

SeaWiFS Postlaunch Technical Report Series

Stanford B. Hooker and Elaine R. Firestone, Editors

Volume 21, The Eighth SeaWiFS Intercalibration Round-Robin Experiment (SIRREX-8), September–December 2001

Giuseppe Zibordi, Davide D'Alimonte, Dirk van der Linde, Jean-François Berthon, Stanford B. Hooker, James L. Mueller, Gordana Lazin, and Scott McLean

National Aeronautics and
Space Administration

Goddard Space Flight Center
Greenbelt, Maryland 20771

December 2002

The NASA STI Program Office ... in Profile

Since its founding, NASA has been dedicated to the advancement of aeronautics and space science. The NASA Scientific and Technical Information (STI) Program Office plays a key part in helping NASA maintain this important role.

The NASA STI Program Office is operated by Langley Research Center, the lead center for NASA's scientific and technical information. The NASA STI Program Office provides access to the NASA STI Database, the largest collection of aeronautical and space science STI in the world. The Program Office is also NASA's institutional mechanism for disseminating the results of its research and development activities. These results are published by NASA in the NASA STI Report Series, which includes the following report types:

- TECHNICAL PUBLICATION. Reports of completed research or a major significant phase of research that present the results of NASA programs and include extensive data or theoretical analysis. Includes compilations of significant scientific and technical data and information deemed to be of continuing reference value. NASA's counterpart of peer-reviewed formal professional papers but has less stringent limitations on manuscript length and extent of graphic presentations.

- TECHNICAL MEMORANDUM. Scientific and technical findings that are preliminary or of specialized interest, e.g., quick release reports, working papers, and bibliographies that contain minimal annotation. Does not contain extensive analysis.

- CONTRACTOR REPORT. Scientific and technical findings by NASA-sponsored contractors and grantees.

- CONFERENCE PUBLICATION. Collected papers from scientific and technical conferences, symposia, seminars, or other meetings sponsored or cosponsored by NASA.

- SPECIAL PUBLICATION. Scientific, technical, or historical information from NASA programs, projects, and mission, often concerned with subjects having substantial public interest.

- TECHNICAL TRANSLATION. English-language translations of foreign scientific and technical material pertinent to NASA's mission.

Specialized services that complement the STI Program Office's diverse offerings include creating custom thesauri, building customized databases, organizing and publishing research results... even providing videos.

For more information about the NASA STI Program Office, see the following:

- Access the NASA SIT Program Home Page at http://www.sti.nasa.gov/STI-homepage.html

- E-mail your question via the Internet to help@sti.nasa.gov

- Fax your question to the NASA Access Help Desk at (301) 621-0134

- Write to:
  NASA Access Help Desk
  NASA Center for Aerospace Information
  7121 Standard Drive
  Hanover, MD 21076-1320

NASA/TM–2002–206892, Vol. 21

SeaWiFS Postlaunch Technical Report Series

Stanford B. Hooker, Editor
NASA Goddard Space Flight Center, Greenbelt, Maryland

Elaine R. Firestone, Senior Scientific Technical Editor
Science Applications International Corporation, Beltsville, Maryland

Volume 21, The Eighth SeaWiFS Intercalibration Round-Robin Experiment (SIRREX-8), September–December 2001

Giuseppe Zibordi, Davide D'Alimonte, Dirk van der Linde, and Jean-François Berthon
JRC/Institute for Environment and Sustainability, Ispra, Italy

Stanford B. Hooker
NASA Goddard Space Flight Center, Greenbelt, Maryland

James L. Mueller
SDSU Center for Hydro-Optics and Remote Sensing, San Diego, California

Gordana Lazin and Scott McLean
Satlantic, Inc., Halifax, Canada

December 2002

ISSN 1522-8789

Available from:

NASA Center for AeroSpace Information
7121 Standard Drive
Hanover, MD 21076–1320
Price Code: A17

National Technical Information Service
5285 Port Royal Road
Springfield, VA 22161
Price Code: A10

Preface

From the beginning of the SeaWiFS calibration and validation program, much emphasis was placed on the refinement of *in situ* measurement protocols, analysis techniques, instrument technology, and calibration. These activities have produced substantial improvements in the accuracy of the bio-optical and atmospheric data sets used for algorithm development and product validation. Another result of these evaluations and associated experiments was the recognition that all aspects of the measurement process need to be examined in detail, even for parameters thought to be well understood and properly characterized. The studies reported in this technical memorandum underscore this realization with the immersion coefficient for irradiance and the cosine response being the cases in point. For example, it is shown here that previous estimates of the immersion coefficients provided with sensors used by the SeaWiFS Project and its collaborators were in error by as much as 12%. The design, execution, and documentation of these investigations required considerable diligence and ingenuity and should lead to similar re-evaluations of other parameters important to calibration and validation activities but assumed to be sufficiently accurate.

Greenbelt, Maryland — C. R. McClain
July 2002

Table of Contents

Table of Contents (*cont.*)

Abstract

This report documents the scientific activities during the eighth SeaWiFS Intercalibration Round-Robin Experiment (SIRREX-8) held at the Center for Hydro-Optics and Remote Sensing (CHORS), the Joint Research Centre (JRC), and Satlantic, Inc. The objectives of SIRREX-8 were to a) quantify the uncertainties associated with measuring the immersion factor with a standard protocol, b) establish if instrument-to-instrument variability prevents the assignment of a set of immersion factors for an entire series of sensors, c) compare average immersion factors obtained from sample OCI-200 radiometers with those provided by Satlantic for the same series of instruments, and d) measure the cosine response of one sensor at CHORS and Satlantic. An overview of SIRREX-8 is given in Chapt. 1, the immersion factor methods used by the participating laboratories are presented in Chapts. 2–4, and the data processing code is documented in Chapt. 5. The cosine response methods and results are presented in Chapt. 6, along with an analysis of the data. A synthesis of the immersion factor results is presented in Chapt. 7 and includes a discussion and conclusion of the effort with respect to the objectives.

Prologue

The purpose of the Sea-viewing Wide Field-of-view Sensor (SeaWiFS) Project at the National Aeronautics and Space Administration (NASA) Goddard Space Flight Center (GSFC) is to obtain valid ocean color data of the world ocean for a five-year period, to process that data in conjunction with ancillary data to meaningful biological parameters, and to make that data readily available to researchers (Hooker et al. 1992). The success of the SeaWiFS mission will be determined by the quality of the ocean color data set and its availability. The culmination of properly executing this responsibility is achieving a radiometric accuracy to within 5% absolute and 1% relative, water-leaving radiances to within 5% absolute, and chlorophyll *a* concentration to within 35% over a range of 0.05–50.0 $\mathrm{mg\,m^{-3}}$ (Hooker and Esaias 1993).

The type and quality of supporting *in situ* optical measurements and analytical protocols for SeaWiFS calibration and validation were drafted at a SeaWiFS workshop in 1990. A central perspective of the workshop was that the significant expense of field work dictates *in situ* observations will accrue over several years from a variety of sources, using different instruments and approaches. These data must be internally consistent, of known and documented accuracy (but within SeaWiFS requirements), and in a form readily accessible for analysis by ocean color scientists. The findings and recommendations of the workshop were presented by Mueller and Austin (1992) and were immediately adopted as the SeaWiFS Ocean Optics Protocols (SOOP).

Although the immediate concerns of the SOOP were the SeaWiFS mission, the capabilities of other potential ocean color sensors were also recognized, with the intent of developing databases that are relevant to long-term future needs. The importance of the SOOP and the accuracy requirements contained therein is well recognized by the broader scientific and commercial ocean color community, as evidenced by the considerable expansion of the original document to accommodate a broader range of measurements, techniques, and sampling considerations (Mueller and Austin 1995, Mueller 2000, and Mueller et al. 2001).

Ensuring the SeaWiFS calibration and validation field data sets are of uniform quality and have an uncertainty less than 5% requires a continuing commitment to quantifying the uncertainties associated with the spaceborne and *in situ* instrumentation. The uncertainties associated with the satellite sensor are not considered here, although it is important to remember that half of the total uncertainty budget is apportioned to the satellite sensor. Assuming the uncertainties combine in quadrature (the square root of the sum of the squares), the allowed uncertainty in the remote and *in situ* optical data is approximately 3.5% for each ($\sqrt{5^2/2}$).

The sources of uncertainty for the ground truth part of the total uncertainty budget have a variety of sources:

1. The measurement protocols used in the field;
2. The environmental conditions encountered during data collection;
3. The absolute calibration of the field radiometers, which must also be traceable to the National Institute of Standards and Technology (NIST);
4. The conversion of the light signals to geophysical units in a data processing scheme; and
5. The stability of the radiometers in the harsh environment they are subjected to during transport and use.

The first step in the process of controlling uncertainties in field data was establishing and publishing the SOOP. The proper application of the SOOP also reduces any unnecessary contributions from environmental effects, but it does not completely remove them—as environmental conditions worsen, which may be unavoidable, uncertainties

inexorably increase. The third source is the most fundamental, because all the others are only quantifiable if the radiometers are properly calibrated. The fourth source is tied to the protocols, but there are separate subjective aspects of data processing which influence the uncertainties and are not completely resolved by a single protocol. The fifth source has elements both outside and within the instrument manufacturer's control (e.g., damage during shipment and inferior quality of electrical components, respectively).

To ensure a thorough investigation of the uncertainties associated with field data, the SeaWiFS Project implemented an ongoing series of specialized field campaigns and round robins to incrementally investigate the aforementioned sources of uncertainty. The objective of both types of data collection was to quantify the levels of uncertainties, and then to establish methods to reduce the uncertainties if they were not in keeping with the total uncertainty budget already established for SeaWiFS, i.e., any uncertainty that was greater than 1–2% would have to be reduced over time (assuming four sources of uncertainty, a quadrature sum of 3.5% requires each has an uncertainty of about 1.8%).

The SeaWiFS Intercalibration Round-Robin Experiment (SIRREX) activity was established to thoroughly investigate many of the uncertainties in field measurements, particularly those associated with the absolute calibration of the optical sensors. The SIRREX activity was always regarded as a series of incremental investigations, and in the progress from SIRREX-1 to SIRREX-3 (Mueller 1993, Mueller et al. 1994, and Mueller et al. 1996, respectively), the uncertainties in calibrations improved from 7–8% to 1–2%. The SIRREX-4 to SIRREX-6 results (Johnson et al. 1996, Johnson et al. 1999, and Riley and Bailey 1998, respectively) showed calibrations at an uncertainty level of approximately 2% was routinely achievable.

Other round robins were undertaken to look at other uncertainty sources. For example, the first SeaWiFS Data Analysis Round Robin (DARR-94) investigated data processing uncertainties and showed differences in commonly used data processing methods for determining primary optical parameters from *in situ* light data were about 3–4% of the aggregate mean estimate (Siegel et al. 1995). The focus of the second DARR (DARR-00) was to determine if these results could be improved (Hooker et al. 2001). In terms of overall spectral averages, many of the DARR-00 intercomparisons were to within 2.5%, and if the processing options were made as similar as possible, agreement to within less than 1% was possible.

Although the aforementioned round-robin activities were extensive, they did not explore all sources of uncertainty in the optical field data, for example, the so-called immersion factor, $I_f(\lambda)$, was not considered. The immersion factor accounts for the change in sensor responsivity when the in-air calibration is applied to in-water measurements. For in-water sensors, the immersion factor is a first-order term when raw data samples are converted to physical units, that is, it appears in the calibration equation at the same order as the calibration coefficient ($I_f = 1$ for above-water sensors at all wavelengths).

The procedures used for determining calibration coefficients were repeatedly investigated in previous SIRREX activities and more recently, and most thoroughly, during SIRREX-7 (Hooker et al. 2002). Although the majority of the work has been conducted with Satlantic, Inc. (Halifax, Canada) ocean color radiance and irradiance series-200 (OCR-200 and OCI-200, respectively) sensors, the results have generalized applicability with many other sensor types. The SIRREX-7 data showed the calibrations done at Satlantic are in close agreement with the SeaWiFS 2% accuracy requirement (which were demonstrated at SIRREX-5 using a smaller number of sensors and a less rigorous investigation).

The primary objective of SIRREX-8 was a detailed investigation of the immersion factor: a) quantify the uncertainties associated with measuring the immersion factor with a standard protocol, b) establish if instrument-to-instrument variability prevents the assignment of a set of immersion factors for an entire series of sensors, and c) compare average immersion factors obtained from sample OCI-200 radiometers with those provided by Satlantic for the same series of instruments. The secondary objective was to measure the cosine response of one sensor at two of the facilities.

To eliminate any chance of bias associated with one group's implementation of the immersion factor measurement protocol, three different facilities participated in the SIRREX-8 activity, and a common set of nine sensors were characterized at each facility. The three groups that participated were the Center for Hydro-Optics and Remote Sensing (CHORS), the Joint Research Centre (JRC), and Satlantic, Inc.

An overview of SIRREX-8 is given in Chapt. 1, the methods used by the participating laboratories are presented in Chapts. 2–4, and the data processing code is documented in Chapt. 5. The two methods used for the characterization of the cosine response are presented in Chapt. 6. A synthesis of the results is presented in Chapt. 7 along with a discussion and conclusion of the effort with respect to the objectives. The science team is presented in Appendix A. A summary of the material presented in each chapter is given below.

1. SIRREX-8 Overview

The primary objective of SIRREX-8 was a thorough inquiry into the uncertainties associated with the general problem of determining the immersion factors for marine radiometers, and restricting the analysis to Satlantic in-water Ocean Color Irradiance 200-series sensors (the so-called OCI-200 instruments). A small team of investigators was assembled to address these points at three different facilities (the diversity in participants assured no one

peculiarity in one of the methods could bias the results). The secondary SIRREX-8 objective was to measure the cosine response of one sensor at two of the participating facilities. Although up to 12 sensors were measured, 9 were rotated through all three facilities. The instrumentation came primarily from two different organizations with differing measurement objectives, so the assembled sensors had a diverse range of calibration histories, ages, intended uses, sensitivities, saturation levels, etc. The diversity in sensors means a significant subset of the results will have a wider applicability to the larger community.

2. The CHORS Immersion Factor Method

The CHORS method for experimentally determining the immersion factor for irradiance sensors is based on the method developed at the Visibility Laboratory for this measurement. It uses tap water and has the following major features: a) it uses a large covered tank with a sensor support system, which places the radiometer well above the turbulence associated with filling and emptying the tank (the volume of water below the sensor is greater than the amount above the sensor) or any perturbations from the bottom of the tank, so the interior of the tank (when covered) is especially *black*; b) it uses a 400 W lamp with a very small filament, so the light source very nearly approximates a point source; and c) it uses an adjustable final baffle to ensure the cone of light illuminating the in-water sensor is as small as possible.

3. The JRC Immersion Factor Method

The JRC measurement system for characterizing the immersion factor of in-water irradiance sensors was based primarily on the implementation of the SeaWiFS Ocean Optics Protocols. It was optimized for the Satlantic 200- and 500-series of radiometers (e.g., the OCI-200, plus the OCR-504 and OCR-507, respectively), but much of the measurement system could be adopted for other instruments with similar diameters (e.g., the OCI-1000). Within the framework of SIRREX-8, the measurement system was used with 12 OCI-200 radiometers: 9 were a common part of the intercomparison experiment, and 3 extra were added because of their specific features. For the latter, one sensor had a very high sensitivity (low saturation level while illuminated), and two had just been purchased (so they had not suffered any degradation from previous field or laboratory exercises). The JRC setup used an optical bench for precise alignment of all the primary components (lamp, baffles, in-water radiometer, and monitoring sensor), demineralized tap water (which ensured, when compared to simple tap water, a better measurement accuracy), and a second storage tank (so the same water could be used for successive measurement sequences).

4. The Satlantic Immersion Factor Method

The measurement system for characterization of the immersion coefficient of the underwater irradiance collectors at Satlantic is based on the implementation of the standard SeaWiFS Ocean Optics Protocols, with measurements performed in seawater. Within the framework of SIRREX-8 the immersion measurements were performed on the nine radiometers from the OCI-200 series, which were part of the intercomparison experiment.

5. Computing the Immersion Factor

The JRC Data Processing System includes a module to support the computation, according to published protocols, of irradiance immersion factors for in-water radiometers. The processing module includes an interface to assist the user in the selection of input and output options (file names and directories), measurement parameters (source-to-collector distance and the refractive index of water), and processing features (the use of dark or background data, or enabling the use of normalization data from a sensor monitoring the light source). Normalization by the monitoring sensor removes additional variance in the measurements caused by light fluctuations from the lamp. The graphic functions of the module are mostly used in displaying data at the different processing stages to immediately flag measurements (for instance, at a single depth) affected by unacceptable perturbations (e.g., light focusing from bubbles in the proximity of the diffusers or noise from a disturbed water surface). The module was used to process all the SIRREX-8 data, thereby ensuring the highest possible intercomparability of $I_f(\lambda)$ values produced for the same set of instruments by the different laboratory methods.

6. Cosine Response Measurements

In addition to the immersion factor characterizations, the cosine response was measured for one irradiance sensor at CHORS and Satlantic (motivated by some preliminary measurements at the JRC). The angular response of an OCI-200 in-water radiometer was characterized by CHORS and by Satlantic using a similar methodology, although the former relied on a point source with a horizontal rotation of the sensor, and the latter relied on a collimated source and a vertical rotation. Results from the analysis of the data from Satlantic show deviations from the ideal cosine response for most of the collectors within, or very close to, the limits suggested by the SeaWiFS Ocean Optics Protocols (i.e., 2% between 0–65° and 10% above 75°). Results obtained from the analysis of the CHORS data show deviations from the ideal cosine response within the suggested limits for the OCI-200 central collector, but consistently higher deviations for the six collectors symmetrically located around the centermost one. The latter result is primarily explained by the use of different sources at the two laboratories (i.e., a lamp at CHORS and a lamp plus a collimator at Satlantic).

7. SIRREX-8 Results, Discussion, and Conclusions

The SIRREX-8 experiment for comparing immersion factors involved nine OCI-200 sensors which were all characterized at three different facilities—CHORS, JRC, and Satlantic—using similar laboratory protocols. One of the

radiometers, E_u S/N 130, was selected as a so-called *reference* sensor and was measured more frequently than the other eight. The analysis of the SIRREX-8 data showed intralaboratory measurement uncertainties, evaluated through multiple characterizations of the reference radiometer and defined by two standard deviations, ranging from 0.28% for Satlantic, and up to 0.49% and 0.60% for JRC and CHORS, respectively. Interlaboratory uncertainties, evaluated with data from the nine common radiometers, showed average unbiased percent differences (UPDs) lower than ±0.6%. The analysis of $I_f(\lambda)$ variability across radiometers of the same series showed average values of approximately 2%, with maximum values of up to 5%, for all three laboratories. Typical $I_f(\lambda)$ values for the OCI-200 series of radiometers were produced with $I_f(\lambda)$ data from measurements taken from the three laboratories.

Chapter 1

SIRREX-8 Overview

Stanford B. Hooker
NASA/Goddard Space Flight Center
Greenbelt, Maryland

Giuseppe Zibordi
JRC/IES/Inland and Marine Waters Unit
Ispra, Italy

Abstract

The primary objective of SIRREX-8 was a thorough inquiry into the uncertainties associated with the general problem of determining the immersion factors for marine radiometers, and restricting the analysis to Satlantic in-water Ocean Color Irradiance 200-series sensors (the so-called OCI-200 instruments). A small team of investigators was assembled to address these points at three different facilities (the diversity in participants assured no one peculiarity in one of the methods could bias the results). The secondary SIRREX-8 objective was to measure the cosine response of one sensor at two of the participating facilities. Although up to 12 sensors were measured, 9 were rotated through all three facilities. The instrumentation came primarily from two different organizations with differing measurement objectives, so the assembled sensors had a diverse range of calibration histories, ages, intended uses, sensitivities, saturation levels, etc. The diversity in sensors means a significant subset of the results will have a wider applicability to the larger community.

1.1 INTRODUCTION

When a cosine collector is immersed in water, its light transmissivity is less than it was in air. Irradiance sensors are calibrated in air, however, so a correction for this change in collector transmissivity must be applied when the in-water raw data are converted to physical units. The correction term is called the immersion factor, and it must be determined experimentally, using a laboratory protocol, for each sensor wavelength, λ.

When the sensor is illuminated, the raw optical data samples at each wavelength are recorded as digitized voltages, $V(\lambda)$, usually in counts. Each sample is recorded at a particular time, t_i, which also sets the depth, z. Raw irradiance data are typically converted to physical units using a calibration equation of the following form:

$$E(\lambda, t_i) \;=\; C_c(\lambda)\, I_f(\lambda)\, \big[V(\lambda, t_i) \;-\; \bar{D}(\lambda)\big], \qquad (1)$$

where $E(\lambda, t_i)$ is the calibrated irradiance, $C_c(\lambda)$ is the calibration coefficient (determined during the radiometric calibration of the sensor), $I_f(\lambda)$ is the immersion factor†, and $\bar{D}(\lambda)$ is the average bias or dark voltage measured during a special *dark cast* with the caps on the radiometer. The difference between $V(\lambda, t_i)$ and $\bar{D}(\lambda)$ is the net signal level detected by the radiometer while exposed to light.

In some cases, dark voltages are replaced by so-called *background* or *ambient* measurements, so illumination biases can be removed along with the dark correction. For the purposes of SIRREX-8, background data were collected with the direct illumination of the target by the source occulted by an intervening *on-axis baffle*, so only indirect light (from the source and any other light emissions from equipment in the room) reached the sensor aperture. Ambient data were collected with the source off, so only illumination from other light-emitting devices in the room reached the sensor aperture.

In the formulation given in (1), the irradiances measured during ocean color field campaigns are usually the in-water downward irradiance, $E_d(z, \lambda)$, the in-water upwelled irradiance, $E_u(z, \lambda)$, and the above-water total solar irradiance, $E_d(0^{+}, \lambda)$. In some data processing schemes (Hooker et al. 2001), there is an explicit attempt to try and get the extrapolated in-water downward irradiance to agree with the measured above-water total solar irradiance over the time period associated with the extrapolation interval, so the application of the immersion factor to the former must be accurate.

† For the purposes of the calibration equation, the immersion factor for an above-water irradiance sensor is always equal to unity.

The reflection and transmission aspects of the immersion factor is described by Mueller and Austin (1995), so only a brief summary is provided here. The net change in the immersed transmissivity of a cosine collector is influenced by two separate processes: a change in the reflection of light at the upper surface, and internal scattering and reflections from the lower surface. Although the majority of light reaching the diffuser material defining the outer surface of the collector passes through the collector and reaches the detector, a small part of the incident light is reflected at the air–plastic, or water–plastic, interface. The relative size of this reflectance, called *Fresnel reflectance,* depends on the relative difference in refractive indices between the diffuser material and the surrounding medium.

The refractive index of the diffuser material is always larger than the refractive index of water, $n_w(\lambda)$, or air, $n_a(\lambda)$. In addition, $n_w > n_a$, so Fresnel reflectance is smaller at a diffuser–water interface than at a diffuser–air interface. The initial transmission of light through the upper surface of an irradiance collector is, therefore, larger in water than in air. The immersed upper surface also reflects less of the upward flux of light within the diffuser (originating from backscattered light within the diffuser body and from light reflected at the lower diffuser–air interface in the interior of the instrument), so a larger fraction of the internally scattered and upwardly reflected light passes back into the water than would be lost into air. Because the increased upward loss of internally reflected light exceeds the gain in downward flux through the diffuser–water interface, the net effect of these competing processes is a decrease in transmissivity for an immersed cosine collector. Consequently, $I_f > 1$ for in-water irradiance sensors.

Although the immersion factor can be computed for radiance sensors (Mueller and Austin 1995), it must be measured for irradiance sensors. An accepted procedure can be generalized with just a few steps. The instrument is placed in a tank of water with the irradiance collector level and facing upward. A tungsten-halogen lamp with a small filament, powered by a stable power supply, is placed at some distance above the water surface. The depth of the water is lowered in steps and readings are recorded for all wavelengths from each carefully measured depth. A final reading is taken with the water level below the collector, i.e., with the collector in the air and completely dry.

To eliminate any bias associated with one particular implementation of the immersion factor protocol, three different facilities participated and nine common instruments were characterized at each facility. The three groups that participated were CHORS (San Diego, California), the JRC (Ispra, Italy), and Satlantic. The details of how each group implemented this method into a protocol for their facility is described in Chapters 2–4, respectively.

Regardless of the methodology employed during the laboratory data collection exercise, there are aspects of the problem that can only be dealt with during the data processing phase of the experiment. The flux of light arriving at the collector varies as a) a function of the transmittance at the air–water interface (which varies with wavelength), b) the attenuation over the water pathlength (which is a function of depth and wavelength), and c) the change in solid angle of the light leaving the source and arriving at the diffuser (caused by the light rays changing direction at the air–water interface, which varies with wavelength and water depth). The data processing scheme to account for these effects is presented in Chapt. 5.

1.2 OBJECTIVES

The primary objective for SIRREX-8 was to make detailed inquiries associated with the determination of the immersion factor:

1. Quantify the uncertainties associated with measuring the immersion factor with a standard protocol,
2. Establish if instrument-to-instrument variability prevents the assignment of a set of immersion factors for an entire series of sensors, and
3. Compare average immersion factors obtained from sample OCI-200 radiometers with those provided by Satlantic for the same series of instruments.

The latter is particularly important, because manufacturers frequently assume many aspects of sensor characterization can be assigned to an entire instrument series.

The secondary objective was to measure the cosine response of one sensor at two of the facilities, CHORS and Satlantic. The motivation for this part of the activity was some preliminary cosine response work done at the JRC. The cosine response for Satlantic in-water irradiance sensors must be measured in water, and CHORS and Satlantic have excellent facilities for this measurement.

1.3 SCHEDULE

To ensure statistical robustness, each participating facility agreed to measure each sensor at least two times. In addition, one sensor was selected as a so-called *reference* which was supposed to be measured every day, or at least three times over the course of the measurement trials at the facility. The *reference* data ensures any daily changes in the implementation of the methods could be quantified. In addition, the *reference* was the sensor selected for the cosine response characterization.

The scheduling for SIRREX-8 at each facility was set primarily by the amount of time needed to execute one sensor trial at a particular facility, times the total number of anticipated trials, plus the time required for the cosine response measurement (if it was to be made). Some groups were participating under contract, so there were limitations on time based on contractual agreements. The overall schedule to complete all the measurements at all three facilities was set primarily by the amount of time needed to ship the needed sensors and equipment to and from the participating groups.

The measurement trials began at the CHORS facility and extended from 28 September to 8 October 2001. The CHORS method permitted at least four sensors to be measured each day, so the daily sequence was to measure the *reference* sensor first, followed by at least three of the other sensors. This procedure allowed all nine sensors to be measured in three days. At the conclusion of the CHORS measurements, each sensor was measured two or more times.

The second set of trials took place at the JRC from 4–15 November 2001. The JRC method allowed for multiple sensor measurements each day, so the *reference* sensor was measured at least once per day. Although there was enough time to measure each sensor at least three times, problems with maintaining water purity and stability resulted in some sensors being measured less than this.

The final trials occurred at Satlantic from 3–21 December 2001. The Satlantic method required the most time, and only one sensor was measured each day (once in the morning and once in the afternoon). Consequently, the *reference* sensor could not be measured each day, so it was measured at the beginning, middle, and end of the measurement time period.

1.4 INSTRUMENTATION

Satlantic OCI-200 sensors were selected for SIRREX-8, because they are compact (so they can be accommodated in relatively small water tanks) and are widely used by the broader ocean color community (so any conclusions derived from their use would have a larger applicability). A summary of the sensors used is presented in Table 1.

Table 1. The radiometers used during SIRREX-8. The manufacturing dates are based on the first time the instruments were calibrated at Satlantic in the configuration they were used for SIRREX-8.

Sensor	*S/N*	*Date*	*Owner (Notes)*
$E_d(\lambda)$	015	September 1994	JRC (oldest)
$E_d(\lambda)$	040	March 1996	NASA
$E_u(\lambda)$†	047	June 1996	NASA (low sat.)
$E_u(\lambda)$	048	June 1996	NASA
$E_d(\lambda)$	050	June 1996	NASA
$E_d(\lambda)$	071	April 1997	JRC
$E_d(\lambda)$	097	June 1998	JRC
$E_u(\lambda)$	098	May 1998	JRC
$E_u(\lambda)$	109	July 1998	NASA
$E_u(\lambda)$	130	July 1999	JRC (reference)
$E_d(\lambda)$†	161	September 2001	JRC (newest)
$E_u(\lambda)$†	162	September 2001	JRC (newest)

†Only measured at the JRC.

Both $E_d(\lambda)$ and $E_u(\lambda)$ sensor types were characterized during SIRREX-8. The reason for selecting both types was an $E_u(\lambda)$ sensor is more sensitive, so its signal-to-noise ratio (SNR) is higher, which also means it can be used with a lower wattage lamp and greater lamp-to-sensor distances. The use of lower wattage lamps is an experimental advantage, because they are more common and less expensive, and they usually have smaller filaments, so the approximation that the lamp is a point source is better satisfied. The use of greater lamp-to-sensor distances significantly improves the point-source approximation and permits two different experimental distances at satisfactory flux (or SNR) levels.

All the irradiance sensors had D-shaped collars fitted to them at a set distance, usually 3.81 cm (1.5 in), from the faceplate (front) of the sensor (Fig. 1). The use of the D-shaped collar ensures the sensor can be mounted at a reproducible location and orientation (Hooker and Aiken 1998).

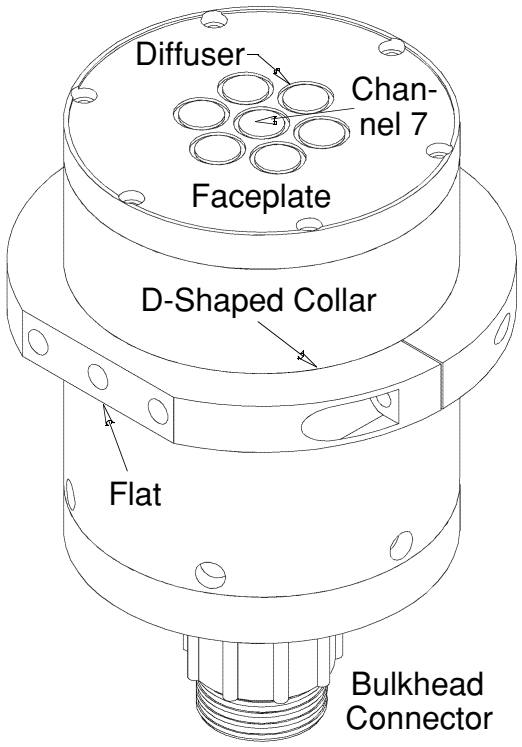

Fig. 1. An OCI-200 (irradiance) sensor fitted with a D-shaped collar. The flat side on the collar has three 1/4 in × 20 taps which can be used, in addition to the collar itself, for fixing the orientation of the sensor in jigs or mounting brackets. Note that channel 7 is the centermost diffuser.

Chapter 2

The CHORS Immersion Factor Method

Stanford B. Hooker
NASA/Goddard Space Flight Center
Greenbelt, Maryland

James L. Mueller
SDSU/Center for Hydro-Optics and Remote Sensing
San Diego, California

Giuseppe Zibordi
JRC/IES/Inland and Marine Waters Unit
Ispra, Italy

Abstract

The CHORS method for experimentally determining the immersion factor for irradiance sensors is based on the method developed at the Visibility Laboratory for this measurement. It uses tap water and has the following major features: a) it uses a large covered tank with a sensor support system, which places the radiometer well above the turbulence associated with filling and emptying the tank (the volume of water below the sensor is greater than the amount above the sensor) or any perturbations from the bottom of the tank, so the interior of the tank (when covered) is especially *black*; b) it uses a 400 W lamp with a very small filament, so the light source very nearly approximates a point source; and c) it uses an adjustable final baffle to ensure the cone of light illuminating the in-water sensor is as small as possible.

2.1 INTRODUCTION

The CHORS laboratory procedure for characterizing immersion coefficients for an irradiance sensor was first described in Petzold and Austin (1988). The apparatus used was designed to accept a large variety of sensor types, both large and small, from different manufacturers. Although measurement accuracy was an important objective of the method, another priority was to be able to execute the measurement process in a time-efficient manner.

2.2 LABORATORY SETUP

The characterization of immersion factors at CHORS took place in a *high-bay* facility adjacent to the room used for radiometric calibrations. The walls and ceiling of the facility were painted flat black to remove any significant sources of reflected or secondary illumination.

A schematic of the CHORS measurement system for measuring $I_f(\lambda)$ for cosine collectors, is shown in Fig. 2. It consisted primarily of a large fiberglass tank in which the radiometer to be characterized could be immersed, a screened 400 W tungsten-halogen lamp with a power supply (PS) and multiple baffles, a reference radiometer to monitor the lamp, and a ducted fan to keep the lamp and reference cooled. The in-water sensor was placed in a support frame on top of a grated platform. The platform was covered with a fine black mesh and provided two functions:

1. It significantly reduced any water turbulance during the filling (and, to a lesser extent, the draining) of the tank; and
2. It provided a horizontal surface which allowed the sensor support frame to be accurately leveled and positioned within the baffled light field.

To reduce light reflections within the tank, the interior was painted with an exterior flat black paint, and the metal surfaces of the grated platform plus the sensor support frame were covered with black tape or black paint. The inside of the tank lid was painted black, and a large opening in the lid was fitted with a black curtain which could be drawn back to permit easy access to the inside of the tank.

The sensor support frame was composed primarily of a tube with an inner diameter just a little larger than the outer diameter of the in-water radiometer. A D-shaped collar was fitted to each in-water sensor which leveled the radiometer against the top of the tube. The flat side of the D-shaped collar (Fig. 1) was used as a coarse alignment reference to ensure the radiometer was positioned in a reproducible fashion within the light field.

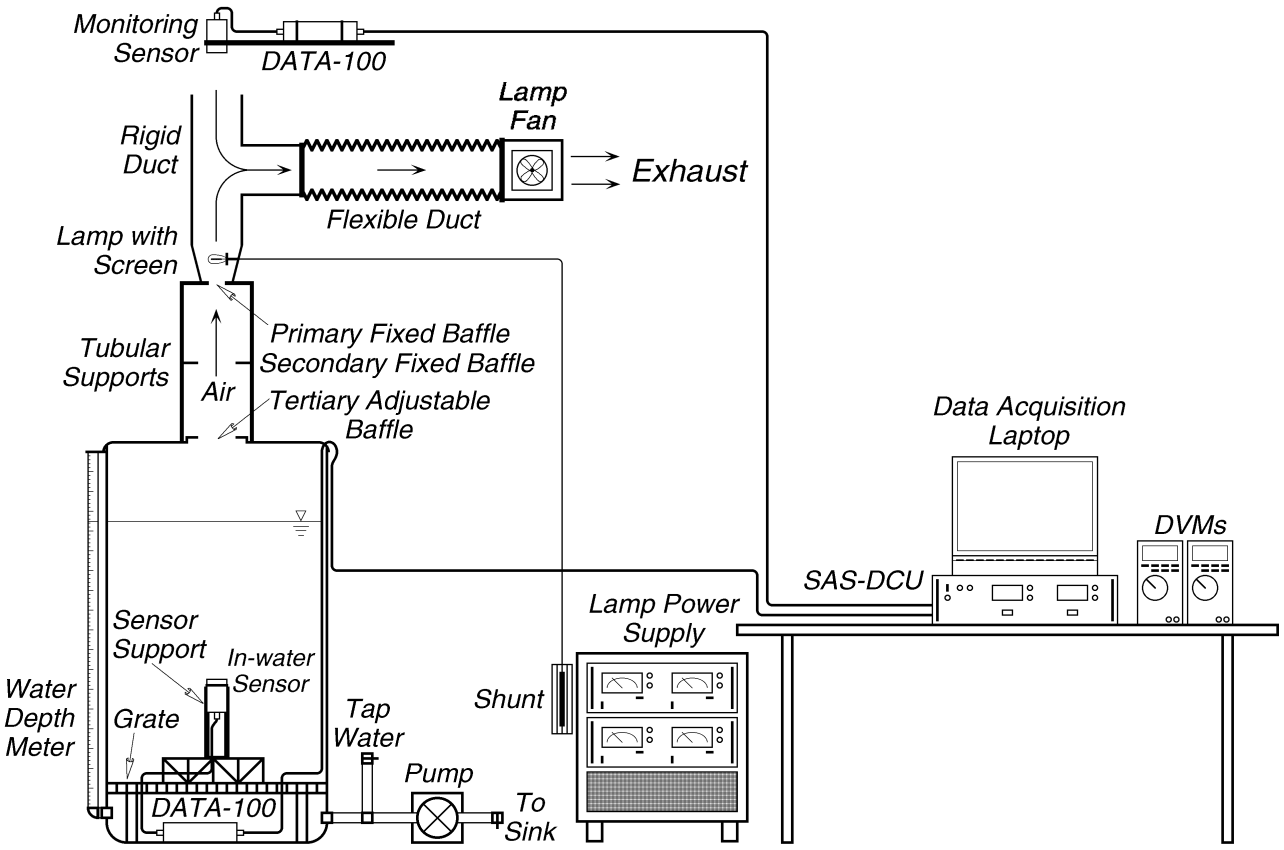

Fig. 2. The laboratory setup used at CHORS for characterizing the immersion factor. The monitoring and in-water sensors are aligned by centering the equipment with respect to the illumination circles associated with the rigid duct and adjustable aperture, respectively.

The lamp was supported on top of a tubular support frame, with primary and secondary baffles, which was attached to the tank lid. The lamp could be positioned at two different positions above the tank, although the lowest position was used most of the time. The lamp had a very small filament, so it very nearly approximated a point source, and it was powered with a regulated Sorenson† power supply. The primary lamp monitor was with the monitoring sensor. A shunt resistor, in series with the lamp, was used as an additional means to monitor the light source stability, which was accomplished by measuring the voltages across the shunt and the lamp with digital voltmeters (DVMs).

Proper alignment of the measurement components with respect to the light field emitted by the lamp was made visually: when the lamp was powered on, the reference and in-water sensor were moved until they were centered within the projected cone of light. The adjustable aperture was adjusted until the diameter of the cone of light within the tank was no larger than the diameter associated with the D-shaped collar.

The tank was filled with tap water through a fitting in the bottom of the tank located below the grated platform. A system of valves allowed the tap water input to be closed, so the tank could be emptied using a pump. The depth of the water was determined by reading the water level on a water depth meter (a clear plastic tube with an attached tape measure) connected to the bottom of the tank.

Two independent Satlantic power-telemetry units (also referred to as *data loggers* and DATA-100s) were used to digitize the analog signals from the in-water and monitoring sensors. A Satlantic 15 V power and data control unit (a so-called SAS-DCU) was used to power the data loggers and convert the RS-485 DATA-100 output into RS-232. A laptop computer and Satlantic ProView software (version 1.0F) were used for data acquisition.

A lamp screen was used to shield the laboratory personnel from the bright light of the lamp, and a small fan was used to keep the lamp screen and monitor sensor cool. The fan was fitted inside the end of a flexible duct which was connected to a rigid duct joined to the lamp holder; the top of the rigid duct was aligned to the monitoring sen-

† Identification of commercial equipment to adequately specify or document the experimental problem does not imply recommendation or endorsement, nor does it imply that the equipment identified is necessarily the best available for the purpose.

sor and the bottom to the lamp holder. The flexible duct allowed the fan to be affixed to any convenient mounting position. The fan pulled air into the duct which ensured air was drawn over the lamp and the faceplate of the monitoring sensor. This had the additional advantage of pulling air up away from the tank, which helped prevent particles from falling into the tank.

The relevant components of the CHORS measurement system are listed in Table 2.

Table 2. The equipment used with the CHORS method for immersion factor characterization.

Device	*Model (S/N)*	*Manufacturer*
Lamp	HLX-64663 36V, 400 W	Ushio
Lamp PS	DCR150-12BM5 (0982)	Sorenson
Monitor	OCI-200 (129)	Satlantic
DATA-100	MVDS (038)	Satlantic
DATA-100	OCP (027)	Satlantic
DATA-100	MVDS Spare (053)	Satlantic
Sensor PS	SAS-DCU (004)	Satlantic
DVM	F-8060A (68520469)	Fluke
DVM	E2378A (3105J12460)	Hewlett-Packard
Shunt	100mv (5945354)	Tepro
Pump	AC-5C-MD (0140541)	March Mfg., Inc.

2.3 MEASUREMENT PROTOCOL

The basic elements of the measurement protocol were the alignment of the mechanical and optical components, and the collection of in-air and in-water data for computing $I_f(\lambda)$. The alignment procedures were as follows:

- The tank lid with attached baffles, lamp holder, and rigid duct were leveled and aligned vertically.
- The lamp was powered on and the monitoring sensor was aligned by centering it in the projected light cone from the top of the rigid duct.
- The in-water sensor was iteratively aligned by centering it in the projected light cone from the light baffles and leveling it using a bullet level.
- The adjustable baffle was set to ensure the outer diameter of the projected light cone matched the outer diameter of the D-shaped collar fitted to the in-water sensor.

Although every effort was made to minimize any perturbation to the alignment when sensors were changed within the tank, some disturbance was inevitable. To ensure alignment integrity over time, occasional alignment checks were made at different periods over the course of the measurements.

The computation of $I_f(\lambda)$ primarily requires one in-air and a multitude of in-water irradiance measurements. The latter must be taken at different water depths, so an accurate determination of the subsurface irradiance value can be made. In addition, dark or ambient data are needed to remove any bias voltages (in a properly baffled setup, these two measurements are almost identical). After setting up the monitoring sensor, the collection of all these data at the CHORS facility requires the following successive steps:

1. The lamp was powered on, by slowly ramping up the applied current until the operational rating was reached, and then the lamp was allowed to warm up for at least 30 min.
2. The in-water radiometer was installed in its support frame (the D-shaped collar ensured an accurate repositioning of the sensors with respect to the system in successive measurement sequences).
3. In-air data from the two light sensors were recorded for 3.0 min, and the DVM voltages were logged.
4. The tank was filled until the water depth above the in-water sensor was 5 cm.
5. While the tank was being filled, any air bubbles that may have formed on, or near, the diffusers were removed.
6. When the tank was filled, the water surface was *skimmed*, i.e., any floating particles or surface scum were removed with a vacuum cleaner (a so-called *wet-dry vacuum*).
7. Data from the in-water radiometer and the monitoring sensor were collected for 3.0 min, and the voltages across the lamp and shunt, as measured by the DVMs, were logged (the latter permit immediate detection of any significant changes in the light source during the experiment).
8. Water was added to the tank in 5 cm increments and data were collected at each interval until the water depth above the in-water sensor was at least 40 cm.
9. Water was pumped out of the tank until the water depth was lowered by approximately 2.5 cm and all data were recorded.
10. Successive pumpings and measurement sequences were repeated at 5 cm intervals until the water depth above the diffusers was approximately 7.5 cm, at which point, a final set of radiometric and DVM measurements were recorded.
11. Water was pumped out of the tank until the water depth was below the D-shaped collar, after which, the diffusers were dried using compressed air and lint-free tissue.
12. Data from the dried in-water radiometer and the monitoring sensor were collected for 3.0 min, and the DVM voltages were recorded.
13. Dark data (caps on the sensors), and then ambient data (caps off and lamp off) were collected.

The final in-air measurement was made so it could be used as a quality control procedure by comparing it to the first in-air measurement. The ambient measurement was also intended to be a quality assurance opportunity, because this measurement included any secondary sources of light in the room. The use of ambient data is preferred over dark data, but (as has already been noted) in a properly baffled measurement system the two should be nearly identical.

Another quality assurance procedure was to use two different lamp-to-sensor distances with the same radiometer (in the alternative lamp position, the lamp is 14.0 cm farther the sensor). Although this was an established part of the CHORS method, it was only executed once during SIRREX-8, because the time available did not permit recurrent use of this procedure.

One complete sequence for characterizing the immersion factor (starting with collecting the dark data, filling and emptying the tank, and then ending with the final in-air measurement), lasted almost 2 h. The most relevant parameters and quantities associated with the CHORS method for characterizing the immersion factor are given in Table 3.

Table 3. The principal parameters defining the CHORS method for characterizing immersion factors.

Parameter	*Value*
Tank size (height×width)	152 cm × 81 cm
Volume of water	780 L
E_d/E_u lamp power	330/330 W
Lamp-to-sensor distance†	86 cm
Maximum water depth	40 cm
Minimum water depth	5 cm
Depth increment	2.5 cm
Number of depths	15
In-air measurement‡	2
Dark measurement§	1
Ambient measurement§	1
Recording time per depth	3.0 min
Total time per sensor trial	∼120 min

† A second distance of 100.0 cm was executed once.
‡ Executed at the start and end of each sensor trial.
§ Executed at the end of each sensor trial.

2.4 DATA COLLECTION

During SIRREX-8, 26 immersion factor characterizations were performed at CHORS, applying the Petzold and Austin (1988) method, for the nine OCI-200 sensors selected as the common instruments. The daily operations always included at least one characterization of S/N 130, which was considered a reference radiometer. The time series of the reference sensor measurements allows for a day-to-day evaluation of any changes in the measurement system during the experiment, and provides a more robust statistical description of at least one sensor.

Table 4 shows the number of measurement trials for each sensor. Only one power level (330 W) was used to power the lamp for both the E_d and E_u radiometers. Although only one current level was used, at least 70 signal counts were achieved in the least sensitive responsivity of each sensor (i.e., specifically in the blue, where both sensor sensitivity and lamp flux are low).

Table 4. The number of measurement trials performed at CHORS, N_T^C, for the different radiometers.

Sensor	*S/N*	N_T^C	*Notes*
$E_d(\lambda)$	015	2	Oldest sensor.
$E_d(\lambda)$	040	2	
$E_u(\lambda)$	048	4	
$E_d(\lambda)$	050	2	
$E_d(\lambda)$	071	2	
$E_d(\lambda)$	097	2	
$E_u(\lambda)$	098	2	
$E_u(\lambda)$	109	2	
$E_u(\lambda)$	130	8	Reference sensor.
	Total	*26*	

2.5 DATA PROCESSING

Data processing for computing the immersion factors was provided by a software module included in the JRC Data Processing System developed for the analysis of field data in support of ocean color calibration and validation activities (D'Alimonte et al. 2001). A complete description of this data processing module is presented in Chapt. 5. A comparison between the usual CHORS data processor and the JRC module showed the two gave nearly identical results.

2.6 SUMMARY

The CHORS method for the characterizing immersion factors for irradiance collectors has the following major features:

1. It uses a large covered tank with a sensor support system, which places the radiometer well above the turbulence associated with filling and emptying the tank (the volume of water below the top of the sensor is greater than the amount above the sensor) or any perturbations from the bottom of the tank, so the interior of the tank (when covered) is especially *black*;
2. It uses a lamp with a very small filament, so the light source very nearly approximates a point source; and
3. It uses an adjustable final baffle to ensure the cone of light illuminating the in-water sensor is as small as possible.

Chapter 3

The JRC Immersion Factor Method

Giuseppe Zibordi
Dirk van der Linde
Jean-François Berthon
JRC/IES/Inland and Marine Waters Unit
Ispra, Italy

Abstract

The JRC measurement system for characterizing the immersion factor of in-water irradiance sensors was based primarily on the implementation of the SeaWiFS Ocean Optics Protocols. It was optimized for the Satlantic 200- and 500-series of radiometers (e.g., the OCI-200, plus the OCR-504 and OCR-507, respectively), but much of the measurement system could be adopted for other instruments with similar diameters (e.g., the OCI-1000). Within the framework of SIRREX-8, the measurement system was used with 12 OCI-200 radiometers: 9 were a common part of the intercomparison experiment, and 3 extra were added because of their specific features. For the latter, one sensor had a very high sensitivity (low saturation level while illuminated), and two had just been purchased (so they had not suffered any degradation from previous field or laboratory exercises). The JRC setup used an optical bench for precise alignment of all the primary components (lamp, baffles, in-water radiometer, and monitoring sensor), demineralized tap water (which ensured, when compared to simple tap water, a better measurement accuracy), and a second storage tank (so the same water could be used for successive measurement sequences).

3.1 INTRODUCTION

The JRC is extensively involved in field measurements to support ocean color calibration and validation activities. To sustain these measurements, and to allow a comprehensive characterization of the equipment used in the field campaigns, a laboratory was established for the absolute calibration of optical instruments. An absolute radiometric calibration requires the capability of tracing instrument response to the appropriate standards laboratory†. For in-water optical instruments, it also requires the capability of characterizing the immersion factor (Tyler and Smith 1970).

Mueller (1995) showed the variability in $I_f(\lambda)$ values within the same radiometer series can be significant, which challenges the notion of class characterizations and suggests individual sensors need to be characterized if uncertainty budgets are to be minimized. Consequently, the JRC devised a measurement system for characterizing the immersion factor, which could be quickly and easily set up in the optical laboratory. The JRC capability is based on the protocol presented by Petzold and Austin (1988) and Mueller and Austin (1995), and has been designed primarily for the irradiance sensors used in the field activities, i.e., the Satlantic 200- and 500-series of ocean color radiometers (the OCI-200, plus the OCR-504 and OCR-507, respectively).

† For SeaWiFS calibration and validation activities, the radiometric scale must be traceable to a NIST scale of spectral irradiance.

3.2 LABORATORY SETUP

The JRC immersion factor characterizations were made inside the same facility used for radiometric calibrations. The primary advantage of this approach was the room was already carefully baffled (with black curtains and flat black wall paint) to remove any significant sources of reflected or secondary illumination. Another advantage was the optical bench used for the calibration measurements was available for precise positioning of the components needed for the immersion factor characterizations. Because compact (OCI-200) sensors were used for SIRREX-8, a relatively small tank system could be set up in the calibration laboratory without negatively influencing the normal use of the laboratory.

The schematic of the JRC measurement system for characterizing $I_f(\lambda)$ for cosine collectors, is shown in Fig. 3. It consisted primarily of a tank in which the radiometer to

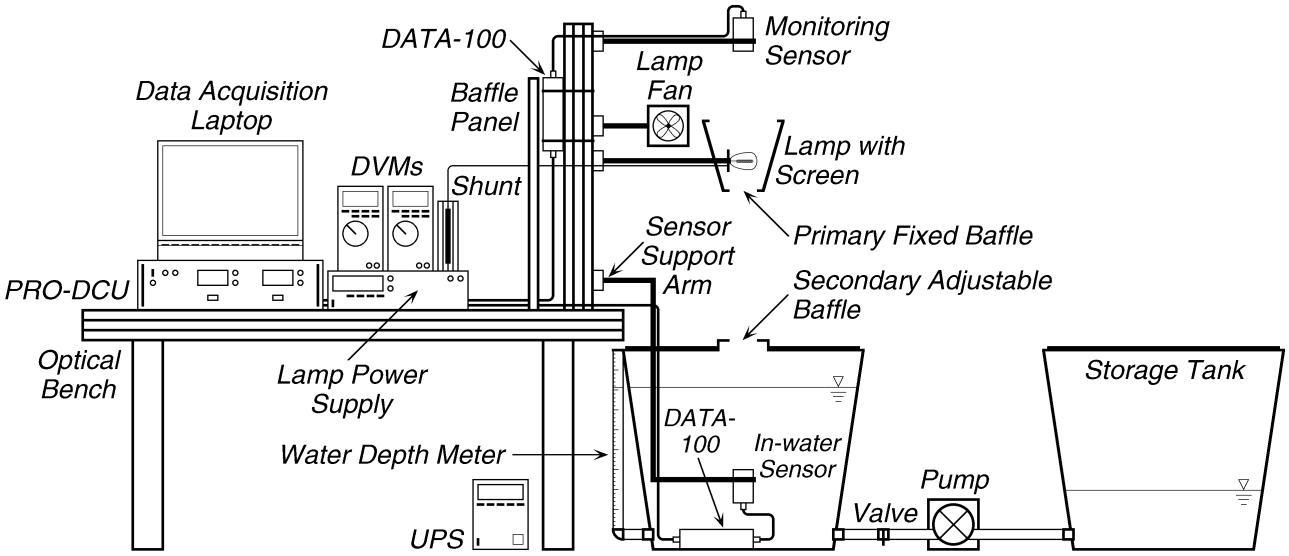

Fig. 3. The laboratory apparatus used at the JRC for characterizing the immersion factor. The PRO-DCU, the lamp power supply, the laptop computer, and the lamp cooling fan were all operated on an uninterruptable power system (UPS). Although only one valve is shown with the pump (for simplicity), the actual system had a valve manifold which permitted a variety of sophisticated tank filling and pumping options.

be characterized could be immersed, and an optical bench. The optical bench was used to support an arm for kinematically mounting the irradiance sensor in the tank, the light source (a relatively small 1,000 W tungsten-halogen lamp), illumination baffles, and a monitoring sensor for the light source. The mechanical support for the in-water radiometer (i.e., specifically the arm connecting the radiometer mount to the optical bench) was designed with the smallest cross-sectional area possible to minimize reflective perturbations within the tank. All of the optical bench components could be quickly and independently positioned with respect to one another.

Proper alignment of the measurement components was made with a laser that was temporarily inserted into the mount for the monitoring sensor or, alternatively, into the mount for the in-water radiometer. A second tank, connected to the first with a hose and pump system, permitted temporary water storage for successive measurement trials (a water valve manifold ensured the selection of proper flow direction and stoppage). The lamp was powered with a regulated Hewlett-Packard, Inc. (HP) power supply. A shunt resistor, in series with the lamp, was used as an additional means to monitor the light source stability. This was accomplished by measuring the voltages across the shunt and the lamp with DVMs.

Two independent data loggers (DATA-100s) were used for the in-water and the monitoring sensors. A Satlantic power and data control unit (PRO-DCU) was used to power the data loggers and convert the RS-485 DATA-100 output into RS-232. A laptop computer and Satlantic ProView software (version 1.0F) were used for data acquisition. A separate large baffle panel isolated the data acquisition and power equipment from the measurement system. A lamp screen was used to shield the laboratory personnel from the bright light of the lamp, and a small fan was used to keep the lamp screen cool. The fan was positioned to also blow away the hot air convecting up from the lamp, which prevented a build up of heat on the monitoring sensor diffusers, and it helped prevent particles from falling down through the adjustable aperture and into the tank.

Demineralized tap water, with a typical resistance of 5–8 MΩ, was used in the measurement system. To further minimize perturbations by ambient light, the two tanks and all mechanical parts composing the system, were black. The relevant components of the measurement system are detailed in Table 5.

Table 5. The equipment used with the JRC method for $I_f(\lambda)$ characterizations.

Device	*Model (S/N)*	*Manufacturer*
Lamp	230V 1,000W F6,3A	Osram
Laser	3 mW 670 nm	Radio Spares
Lamp PS	6010A (37110281)	HP
Monitor	OCI-200 (129)	Satlantic
DATA-100	MVDS† (038)	Satlantic
DATA-100	OCP‡ (027)	Satlantic
DATA-100	MVDS† Spare (053)	Satlantic
Sensor PS	PRO-DCU (048)	Satlantic
DVM	F-189 (78150600)	Fluke
DVM	F-87III (70560873)	Fluke
Shunt	1282–0.01 (201677)	Burster
Pump	63/2 (10826)	SB

† Multichannel Visible Detector System.
‡ Ocean Color Profiler.

3.3 MEASUREMENT PROTOCOL

The basic elements of the measurement protocol were the alignment of the mechanical and optical components, and the collection of in-air and in-water data for computing $I_f(\lambda)$. The alignment procedures were as follows:

- Each component connected to the optical bench (i.e., the monitoring radiometer mount, the lamp holder, the primary baffle, and the in-water radiometer mount) were leveled;
- The monitoring sensor mount, the lamp filament, the primary baffle, and the in-water radiometer mount were aligned using a 3 mW laser (the laser was mechanically centered using an adapter placed in the monitoring sensor mount); and
- The main tank was centered with respect to the axis of the optical system.

Although some steps were executed more than once (usually in an iterative fashion), the overall alignment was performed only once, because none of the mechanical parts constituting the measurement system were moved during the installation or removal of the radiometers as they were individually measured. To ensure alignment integrity over time, however, occasional alignment checks were made at different periods over the course of the entire experimental activity.

The computation of $I_f(\lambda)$ primarily requires one in-air and several in-water irradiance measurements. The latter must be taken at different water depths, so an accurate determination of the subsurface irradiance value can be made. In addition, dark or background data are needed to remove any bias voltages. The collection of all these data, after setting up the monitoring sensor, requires the following successive steps:

1. The lamp was powered on, by slowly ramping up the applied current until the operational rating was reached, and then the lamp was allowed to warm up for at least 30 min.
2. The in-water radiometer was installed in its mount (the D-shaped collar ensured accurate repositioning of the device with respect to the system in successive measurement sequences).
3. The tank was filled until the water depth above the in-water radiometer was (typically) 35 cm.
4. While the tank was being filled, any air bubbles that may have formed on or near the diffusers were removed.
5. When the tank was filled, the water surface was *skimmed*, i.e., any floating particles or surface scum were removed with a wet-dry vacuum.
6. The secondary adjustable baffle was aligned by visually checking the symmetry of the projected light from the lamp onto the D-shaped collar attached to the in-water radiometer. The adjustable aperture opening was chosen such that the projected light circle overfilled the front face of the radiometer, but was confined to the diameter of the D-shaped collar (i.e., the light circle typically covered an area identified by a radius approximately 1 cm larger than the radius of the radiometer).
7. Data from the in-water radiometer and the monitoring sensor were collected for about 1.5 min, and the voltages across the lamp and shunt, as measured by the DVMs, were logged (the latter permit immediate detection of any significant changes in the light source during the experiment).
8. Water was pumped out of the tank until the water depth was lowered by approximately 2.5 cm, at which point, above- and in-water data were collected for about 1.5 min (and the DVM voltages were recorded).
9. Successive pumpings and measurement sequences were repeated in 2.5 cm increments until the water depth above the diffusers was approximately 5 cm, at which point, a final set of radiometric and DVM measurements were recorded.
10. Water was pumped out of the tank until the water depth was below the D-shaped collar, after which, the diffusers were dried using compressed air and lint-free tissue.
11. Data from the in-water radiometer (now dry, so the measurement sequence was for the needed in-air data) and the monitoring sensor were collected for about 1.5 min, and the DVM voltages were recorded.
12. In addition to dark measurements, taken with caps on the monitoring and in-water radiometers, an on-axis, circular baffle (a small circular disk supported by very thin rods affixed to a larger circular base) was placed above the in-water radiometer by resting it on the D-shaped collar, so background data could be collected; data from the radiometers were collected for 1.5 min and the DVM voltages were logged.

The on-axis baffle was designed to occult the area occupied by the cosine collectors. It had a bottom support ring which fit over the radiometer and rested on the D-shaped collar, so it could be used quickly and easily within the covered tank.

The background measurement was intended to include the contribution of internal reflections from the tank walls and from the mechanical supports. The use of background data is preferred over dark data, but (as has already been noted) in a properly baffled measurement system, the two should be nearly identical.

One complete characterization sequence (starting with filling the tank and ending with the dark and background measurements), typically lasted about 100 min (approximately 20 min was needed to fill the tank and about 40 min

was needed for the in-water measurements). The most relevant parameters and quantities associated with the JRC protocol for characterizing the immersion factor is given in Table 6.

Table 6. The principal parameters defining the JRC method for characterizing immersion factors.

Parameter	*Value*
Tank size (height×width)†	70 cm × 80 cm
Volume of water	350 L
E_d/E_u lamp power	760/880 W
Lamp-to-sensor distance	105 cm
Maximum water depth	35 cm
Minimum water depth	5 cm
Depth increment	2.5 cm
Number of depths	13
In-air measurement‡	1
Dark measurement‡	1
Background measurement‡	1
Recording time per depth	1.5 min
Total time per sensor trial§	∼100 min

† The width is the average internal diameter.
‡ Executed at the end of each sensor trial.
§ Includes about 20 min to fill the tank.

3.4 DATA COLLECTION

During SIRREX-8, 35 measurement sequences (i.e., different characterizations of I_f) were performed with the described system. These included multiple characterizations of the nine OCI-200 sensors selected as the common sensors for the experiment, plus the characterization of three different OCI-200 sensors which were added because of some special feature (i.e., S/N 047 for its high sensitivity plus S/N 161 and 162 because of their noncontamination by any previous field or laboratory deployment). The S/N 130 sensor was considered a reference radiometer, and it was characterized at least once every day to track changes in the measurement system during the experiment.

Table 7 shows the number of measurement trials for each sensor. Two different power levels were used to power the lamp for the E_d and E_u radiometers (i.e., 760 and 880 W, respectively). This was suggested by the need for optimizing the irradiance levels as a function of the sensitivity of the radiometer type and to ensure collection of data with at least 100 signal counts (i.e., specifically in the blue part of the spectrum, where both sensor sensitivity and lamp flux are low). Remember that each depth value used in the $I_f(\lambda)$ computations results from the averaging of 1.5 min of data collected at 6 Hz (i.e., from the averaging of approximately 540 samples), and that the uncertainty decreases with the inverse square root of the number of samples, the highest digitization uncertainty is always expected to be less than 0.04%.

Table 7. The number of measurement trials performed at the JRC, N_T^J, for the different radiometers.

Sensor	*S/N*	N_T^J	*Notes*
$E_d(\lambda)$	015	2	Oldest sensor.
$E_d(\lambda)$	040	2	
$E_u(\lambda)$	047	1	Most sensitive sensor.
$E_u(\lambda)$	048	3	
$E_d(\lambda)$	050	2	
$E_d(\lambda)$	071	4	
$E_d(\lambda)$	097	3	
$E_u(\lambda)$	098	2	
$E_u(\lambda)$	109	4	
$E_u(\lambda)$	130	10	Reference sensor.
$E_d(\lambda)$	161	1	Newest sensor.
$E_u(\lambda)$	162	1	Newest sensor.
	Total	*35*	

During the entire experiment, a major effort was made to ensure the highest possible purity of water. This was accomplished by partially or completely replacing the water in the tank every 2–3 days. In fact, contamination by the hoses, the tanks themselves, the pump, and airborne particles, were producing a reduction in the original quality of the water as a function of time. Screening of measurement sequences significantly affected by a reduced purity of water is recommended by applying a threshold to the diffuse attenuation coefficient $K(\lambda)$ computed with the in-water data (i.e., the negative slope from the linear regression as a function of water depth of the logarithm of in-water data corrected by the geometric perturbations due to the finite distance of the point source).

3.5 DATA PROCESSING

Data processing for computing the immersion factors was provided by a software module included in the JRC Data Processing System developed for analyzing field data in support of ocean color calibration and validation activities (D'Alimonte et al. 2001). A complete description of this data processing module is presented in Chapt. 5.

3.6 SUMMARY

The basic JRC measurement system for characterizing immersion factors for irradiance collectors has the following major features:

1. It uses an optical bench to hold all the supports for the parts to be aligned (lamp, primary baffle, in-water radiometer, and monitoring radiometer), which firmly affixes the mechanical orientation of the system and simplifies alignment procedures, particularly when different setups are required (i.e., different distances among the various subcomponents).

2. It uses demineralized tap water which provides, in comparison to simple tap water, a better measurement accuracy by reducing the perturbative effects of suspended particles. (A storage tank allows for reusing the water in successive measurement sequences.)

Within the framework of SIRREX-8, multiple characterizations of 12 OCI-200 radiometers (i.e., the 9 required by the experiment and the additional 3 with special features) were carried out, for a total of 35 measurement sequences. The use of a threshold applied to the diffuse attenuation coefficient $K(\lambda)$ resulting from the regression analysis of in-water data, was used as a water quality indicator to remove measurement sequences affected by a decreased quality of the water from aging and contamination.

Chapter 4

The Satlantic Immersion Factor Method

Gordana Lazin
Scott McLean
Satlantic, Inc.
Halifax, Canada

Abstract

The measurement system for characterization of the immersion coefficient of the underwater irradiance collectors at Satlantic is based on the implementation of the standard SeaWiFS Ocean Optics Protocols, with measurements performed in seawater. Within the framework of SIRREX-8 the immersion measurements were performed on the nine radiometers from the OCI-200 series, which were part of the intercomparison experiment.

4.1 INTRODUCTION

Satlantic, as a manufacturer of optical instruments, has performed immersion measurements as an instrument class characterization as specified in the original SeaWiFS protocols (Mueller and Austin 1995). The methodology for immersion measurements implemented at Satlantic is the standard method outlined in the SeaWiFS protocols (Mueller and Austin 1995). At Satlantic, different variations of immersion methodologies have been carefully studied and intercompared in the past and the standard method was chosen for community consensus. The results of those studies show that the immersion measurements at Satlantic are highly repeatable (within 0.5%) with the similar level of uncertainties. The main distinction from other laboratories determining immersion factors is that Satlantic uses filtered seawater† instead of commonly used fresh water.

To date, the immersion measurements, protocols, and results from Satlantic have never been intercompared with other laboratories. The SIRREX-8 activities represent an extremely valuable opportunity for evaluation of quality and accuracy of immersion measurements.

4.2 THE MEASUREMENT SYSTEM

The measurement of immersion coefficients in Satlantic are performed in a large black water tank designed to accommodate various underwater optical tests and instrument sizes. The experimental setup for the immersion measurements is shown in Fig. 4 and the equipment used is itemized in Table 8.

The irradiance sensor is mounted on the vertical rail inside the tank with the irradiance collector level facing upward, and is able to slide up and down. A stable light source (1,000 W tungsten-halogen FEL lamp) is placed at the desired distance directly above the instrument. The instrument and lamp alignment is achieved using a laser that is mounted on the rail above the lamp, and removed before measurements. The measurement tank is connected with the water-storage tank by a system of pipes and a pump that enables water transfer between the tanks. Each time the water is transferred between the tanks, it passes through 1 µm filter that is incorporated in the pipeline design. The water level in the measurement tank is determined with a precision of ±0.5 mm using graduated water-meter tube mounted on the side. During measurements, the tank is covered by black covers, except for the aperture underneath the lamp for illumination of the instrument. The radiometer for monitoring lamp stability is mounted on the side of the tank looking, at the side of the lamp. The monitoring radiometer is not a standard protocol for Satlantic immersion measurements and was used to accommodate SIRREX-8 recommendations.

For 200-series heads characterized during SIRREX-8, the data logger was fixed to the vertical rail in the tank and connected by cable to the OCI-200 head mounted in the rings. The monitoring radiometer used a separate data logger, powered from the same power supply as the in-water instrument. The lamp, in the series with a shunt resistor, was powered by a stable digital power supply. The data were logged using Satlantic data acquisition software (SatView). To minimize any perturbation from ambient

† The water is originally from Halifax Harbour, pumped at the Dalhousie University through a series of sand filters, and then brought to the Satlantic calibration facility.

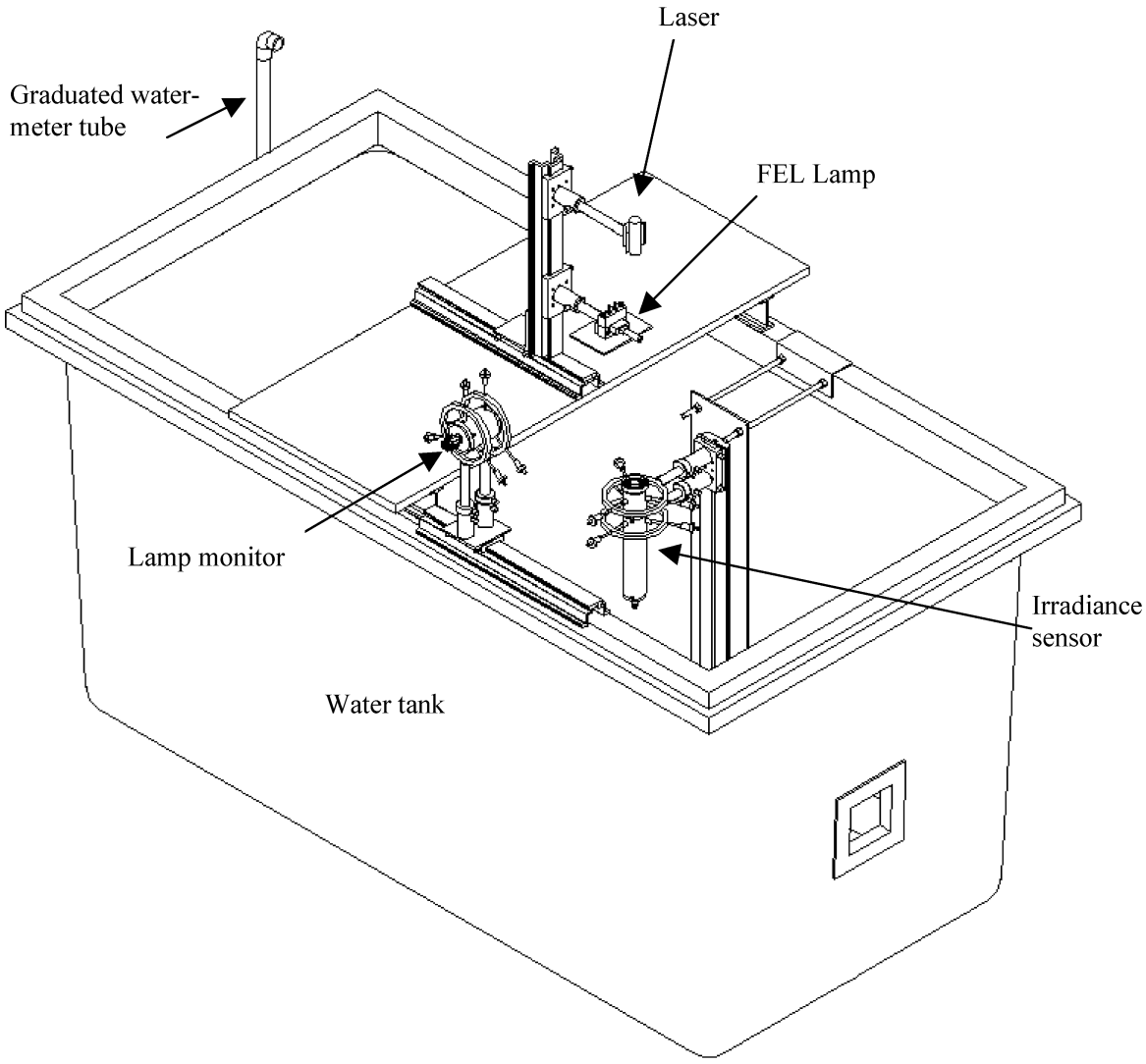

Fig. 4. The experimental setup for immersion factor measurements used at Satlantic.

light, all the mechanical parts were black and the experiment was performed in the dark room.

The water used in the measurements is highly filtered seawater with the periodic (every 2 months) addition of a small amount of chlorine, and its optical properties were evaluated in the past using AC-9 measurements. The results showed low scattering ($c \approx a$) and increased absorption in blue what indicates the presence of dissolved organic matter.

Table 8. The equipment used for immersion measurements at Satlantic.

Device	*Model (S/N)*	*Manufacturer*
Lamp	FEL (F-639)	OL†
Alignment Laser	1 mW 650 nm (2045)	Melles Griot
Lamp PS	OL83 (99115110)	OL†
Monitor	OCI-200 (129)	Satlantic
DATA-100	MVDS (000)	Satlantic
DATA-100	MVDS (053)	Satlantic
Sensor PS	E3631A (KR75310713)	Hewlett-Packard
Shunt	Custom Made	Satlantic‡
Pump	BPND (1C93G)	Berkley/Wicor

† Optronic Laboratory. ‡ Calibrated by Pylon.

4.3 MEASUREMENT PROTOCOL

The measurement protocol consists of three main steps: system alignment, distance setup, and data collection. Each of the steps is described below.

Since the rails are permanently mounted in the tank the system alignment procedure consists from aligning the lamp and the instrument using the diode laser as following:

A. The laser is mounted on the vertical rail above the lamp holder and aligned by using the reflection of its own beam from the water surface.

B. The lamp alignment jig is placed in the lamp holder and aligned so that the laser hits the center of the lamp alignment jig and reflects back into itself.

C. The instrument is mounted in the rings on the vertical rail in the tank with the laser beam hitting the middle of the central diffuser. To ensure that the front surface of the sensor is horizontal an oversized cap with a mirror is placed on the sensor's front surface and the instrument is aligned using laser reflection from the mirror.

D. The radiometer for lamp monitoring is aligned visually and its alignment is not disturbed during whole experiment.

Once the alignment is achieved, the tank is filled with highly filtered seawater. The filling of the tank takes approximately one hour at the rate of about 2 cm min^{-1} (55 L min^{-1}). The filling process introduces many bubbles into the water, which strongly increase the in-water scattering. Therefore, before starting the measurements, three to four hours were allowed for bubbles to dissipate.

Measurement of the distances between the lamp, instrument, and water surface are determined as follows:

- The initial lamp–surface distance is set to 50 cm and is carefully measured by a ruler from the water surface to the front face of the lamp alignment jig placed in the lamp holder.
- The initial instrument–surface distance (starting depth) is carefully determined using a ruler and adjusting the instrument location on the in-water optical rail. The commonly used starting depth in Satlantic is 50 cm, which makes a lamp–instrument distance of 100 cm†. Any possible bubbles that may have formed on the instrument are removed before the instrument is placed in final position.
- The initial water level in the tank is recorded from the graduated water-meter tube.

Once the lamp–surface distance for a certain water level is determined, the lamp position and the initial water level are kept fixed for all of the casts during the experiment, and only instrument to surface distance is measured for each cast.

Before the data collection, the tank is covered by black covers except for a square aperture between lamp and the sensor. The aperture is such that the source overfills the sensor. The measurement procedure is following:

1. The lamp is powered on and warmed up for at least 20 min.
2. The data are collected using SatView in 1.5 min files, starting at a water surface to instrument depth of 50 cm, ending at depth of 5 cm, in 5 cm decrements as the water depth is lowered with the instrument position fixed. The depth is determined from graduated water meter tube. The logging of in-water data as well as lamp monitor data is done simultaneously.
3. Before collecting each file the water surface is cleared of any particles that might have accumulated by touching the water surface above the sensor with a very small amount of liquid detergent. The detergent changes the surface tension of the water and drives the particles away from the contact point, aggregating them at the edges of the tank and thus reducing measurement variability due to any surface contamination‡.

† The effect of different lamp–instrument distances has been evaluated in the past, and it was found that the different distances do not affect the final result.

‡ When a small amount of soap is added to the water, the soap molecules spread on the water surface to a mono-molecular layer. In the limiting case of a layer thickness much smaller than the wavelength of visible light, the soap layer does not modify the transmittance of the water surface and consequently does not perturb the measurement.

4. After all in-water data are collected the water level is lowered below the sensor level and the diffusers are dried out before in-air data are collected.
5. Dark data are collected with caps on the radiometer for both the monitoring radiometer and the underwater radiometer.

If replicate measurements are required (usually three casts in total are done), the tank is filled up to the original water level, the depths and the distances are rechecked, and the replicate cast is performed. The time required to complete measurements for one cast is about 1 h. With additional time for alignment (20 min), tank filling (1 h), and water settling time (3–4 h), the total time required for one cast is about 5.5 h. That limits the measurement rate to two casts per day. The most relevant parameters and quantities involved in immersion measurements are listed in Table 9.

Table 9. The quantities and parameters involved in immersion measurements at Satlantic.

Parameter	*Value*
Tank size (height×width)†	90 cm × 123 cm
Volume of water‡	3,527 L
Water temperature	22°C
Water salinity	34 ppt
Lamp power	1,000 W
Lamp-to-sensor distance	100 cm
Maximum water depth	50 cm
Minimum water depth	5 cm
Depth increment	5 cm
Number of depths	10
In-air measurement	1
Dark measurement	1
Recording time per depth	1.5 min
Total time per sensor trial§	∼330 min

† The length is 245 cm.

‡ Filtered (1 μm) seawater.

§ Includes at least 300 min for tank filling and settling.

4.4 DATA COLLECTION

The SIRREX-8 immersion measurements at Satlantic were carried out from 3–21 December 2001. The immersion characterization was performed on nine OCI-200 irradiance sensors in this intercomparison round robin. The list of the sensors and the number of casts is given in Table 10. In this experiment, two casts were performed for each radiometer instead of three as required by Satlantic procedure. The reason was insufficient time during the experiment to complete full measurement sequence for each radiometer. The exception was E_u sensor S/N 130, which was considered a reference radiometer and was measured six times on three different days (in the beginning, middle, and in the end of the whole experiment). Since, in general, the repeatability of the immersion measurements is very high at Satlantic (within 0.5%) the two casts per radiometer were considered appropriate otherwise, the measurements during SIRREX-8 were done according to the standard Satlantic procedure and not modified in any way, with the exception of adding a lamp monitoring radiometer to the system.

Table 10. The number of measurement sequences performed for the different radiometers at Satlantic, N_T^S.

Sensor	*S/N*	N_T^S	*Notes*
$E_d(\lambda)$	015	2	Oldest sensor.
$E_d(\lambda)$	040	2	
$E_u(\lambda)$	048	2	
$E_d(\lambda)$	050	2	
$E_d(\lambda)$	071	2	
$E_d(\lambda)$	097	2	
$E_u(\lambda)$	098	2	
$E_u(\lambda)$	109	2	
$E_u(\lambda)$	130	6	Reference sensor.
	Total	*22*	

4.5 DATA PROCESSING

The computation of immersion factors is accomplished using a custom software package which implements the algorithm described in Mueller and Austin (1995). For SIRREX-8, the immersion factors for the Satlantic data set were computed using a software module included in the JRC Data Processing System developed for the analysis of field data in support of ocean color calibration and validation activities (D'Alimonte et al. 2001). A complete description of this data processing module is presented in Chapt. 5.

4.6 SUMMARY

The measurement system at Satlantic for characterization of immersion coefficients for irradiance collectors has the following features:

- Very large water tank (3,500 L) designed to accommodate various kinds of underwater optical tests and instruments, with permanent rail system, simple alignment procedure, and flexible setups.
- Uses highly filtered seawater as the closest approximation to the common deployment environment of the instruments.
- High repeatability and low uncertainties of the measurements.

Chapter 5

Computing the Immersion Factor

Davide D'Alimonte
Giuseppe Zibordi
JRC/IES/Inland and Marine Waters
Ispra, Italy

Abstract

The JRC Data Processing System includes a module to support the computation, according to published protocols, of irradiance immersion factors for in-water radiometers. The processing module includes an interface to assist the user in the selection of input and output options (file names and directories), measurement parameters (source-to-collector distance and the refractive index of water), and processing features (the use of dark or background data, or enabling the use of normalization data from a sensor monitoring the light source). Normalization by the monitoring sensor removes additional variance in the measurements caused by light fluctuations from the lamp. The graphic functions of the module are mostly used in displaying data at the different processing stages to immediately flag measurements (for instance, at a single depth) affected by unacceptable perturbations (e.g., light focusing from bubbles in the proximity of the diffusers or noise from a disturbed water surface). The module was used to process all the SIRREX-8 data, thereby ensuring the highest possible intercomparability of $I_f(\lambda)$ values produced for the same set of instruments by the different laboratory methods.

5.1 INTRODUCTION

The JRC Data Processing System was developed for formatting, calibrating, and processing field and laboratory measurements collected to support ocean color calibration and validation activities (D'Alimonte et al. 2001). Among the functions provided by the package, there is a calibration tool which supports the absolute radiometric calibration of optical instruments. A specific module for the computation of immersion factors for in-water irradiance sensors was implemented in agreement with the method proposed by Tyler and Smith (1970), modified by Petzold and Austin (1988), and then proposed as a standard protocol by Mueller and Austin (1995).

The immersion factor module was written in the Interactive Data Language (IDL) programming environment from Research Systems, Inc. (Boulder, Colorado) to take advantage of its graphical capabilities for data visualization and presentation. The graphic functions are mostly used in displaying data at the different processing stages to immediately flag measurements (for instance, at a single depth) affected by unacceptable perturbations (e.g., light focusing from bubbles in the proximity of the diffusers or noise from a disturbed water surface).

The data processing is supported by a graphical user interface (GUI) which assists the user in selecting input and output options (file names and directories), measurement parameters (source-to-collector distance and the refractive index of water), and processing features (the use of dark or background data, or enabling the use of normalization data from a sensor monitoring the light source).

To remove any extra uncertainty in the computation of immersion factors from different data processors, the JRC immersion factor module was used to compute $I_f(\lambda)$ values for all the data collected during SIRREX-8. This is an important point, because previous round-robins demonstrated that differences in data processors can contribute significantly to the final uncertainty in derived parameters (Hooker et al. 2001).

5.2 PROCESSING REQUIREMENTS

The software module for computing $I_f(\lambda)$ values requires a specific coding for the data file names. In fact, the file names are used to identify the sensor type (E_u or E_d), the sensor serial number, the type of data (dark, background, in-air, or in-water radiometric measurements), the water depth (for the in-water measurements), and the sequential index (in case of multiple measurement sequences for the same sensor within the same laboratory exercise). Specifically, files for computing $I_f(\lambda)$ may contain the following measurement types:

1. Dark data (taken with caps on both of the radiometers);

2. Background data (taken with the direct light from the source blocked by an on-axis baffle placed over the in-water sensor only) or ambient data (taken with the source off and keeping the same secondary illumination conditions existing during the measurement sequence);
3. In-air data (taken with the cosine collectors dry); and
4. In-water data (taken with the cosine collectors at different water depths).

For all these measurement types, the linear distance between the source and the cosine collectors is kept constant (which is a requirement for the immersion factor data processing module).

Dark, background (or ambient), and in-air data files use `IINNNMS.EXT` for the naming convention, which is decoded based on the following:

`II` Indicates the instrument type (`EU` or `ED`),

`NNN` Is the serial number (e.g., `130`),

`M` Sets the measurement type (`D` for dark data, `B` for background or ambient data, and `A` for in-air data),

`S` Is an alphabetic sequence indicator for the specific instrument (i.e., `A` for the first trial, `B` for the second trial, `C` for the third trial, etc.), and

`EXT` Is the file extension.

Data files for the in-water measurements are identified by a slightly different naming convention: `IINNNM_ZZZ.EXT`, where the additional `ZZZ` code indicates the water depth in millimeters (i.e., `350` indicates 350 mm of water above the cosine collectors).

The file extension is used to distinguish between measurements from the in-water radiometer and those from the sensor monitoring the source. The data files from the in-water and monitoring sensor, are taken at the same time, and have the same file name prefix, but they are stored with different file name extensions: the `OCP` extension was used to identify data from the in-water radiometer, and the `MVD` extension was used to identify data from the monitoring sensor. (The `OCP` and `MVD` codes are used by Satlantic to distinguish between in-water and above-water DATA-100s, respectively.)

In the JRC Data Processing System, the routine ingesting the input files has the capability to automatically handle different data formats. During SIRREX-8, most of the data were collected using SatView (version 1.0F) and its output data format was used as the reference format for data storage and processing.

Each data file is composed of a solitary header line, which identifies the contents of each column in the ensuing data records. Temporal information is required for the normalization of the in-water radiometric data with the data from the monitoring sensor, and appears at the end of each data record (the temporal parameters are split between a date stamp and a time stamp). A sample data file for the reference radiometer (E_u sensor S/N 130) is presented in Fig. 5.

```
EU(411.5)...EU(682.7) SAMPLES(AVERAGED)
FRAME(COUNTER) CHECK(SUM) DATETAG TIMETAG2⟨cr⟩
33781...44815 1 60 152 2001308 152311640⟨cr⟩
33781...44815 1 61 156 2001308 152311860⟨cr⟩
33781...44814 1 62 155 2001308 152312030⟨cr⟩
33782...44815 1 63 147 2001308 152312190⟨cr⟩
33781...44813 1 64 156 2001308 152312350⟨cr⟩
```

Fig. 5. A sample data file for E_u sensor 130, with the explicit carriage returns indicated by $\langle cr \rangle$. The `DATETAG` variable is decoded as `YYYYDDD`, where `YYYY` is the year, and `DDD` is the sequential day of the year (SDY). The `TIMETAG2` variable is decoded as `HHMMSSsss`, where `HH` is the hour of the day, `MM` is the minutes of the hour, `SS` is the seconds of the minute, and `sss` is the milliseconds of the second.

5.3 COMPUTING I_f

The average values of the dark and background (or ambient) data records in each file are used for analyzing in-water and in-air irradiance data. The in-air $E(0^+, \lambda)$ and in-water $E(z, \lambda)$ data, required for the $I_f(\lambda)$ determination at wavelength λ, are the averages of all records in each specific file computed after subtracting the average dark (or background) values. When the normalization option is chosen, the in-air and in-water data (after dark or background correction) are divided by the corresponding data from the monitoring sensor (the matchup is based on time), which are then multiplied by the monitoring radiometer data taken at time t_0 (where t_0 is the time of the first record of the in-air measurement data file).

The normalization is calculated before the averages at each depth are computed, and reduces the uncertainties caused by changes in the flux of the light source during the measurement sequences. The number of data files collected with different water depths is not predefined, so all available data files contribute to the computation of the subsurface data.

In agreement with Mueller and Austin (1995), the immersion factor, $I_f(\lambda)$, results from

$$I_f(\lambda) \;=\; \frac{E(0^+, \lambda)}{E(0^-, \lambda)}\, T_s(\lambda), \tag{2}$$

where $E(0^+, \lambda)$ is the in-air irradiance, $E(0^-, \lambda)$ is the subsurface irradiance, and $T_s(\lambda)$ is the transmittance of the water surface to downward irradiance. The latter is given by

$$T_s(\lambda) \;=\; \frac{4 n_w(\lambda)}{\big(1 + n_w(\lambda)\big)^2}, \tag{3}$$

where $n_w(\lambda)$ is the refractive index of water. Relevant to the determination of $I_f(\lambda)$ is the computation $E(0^-, \lambda)$

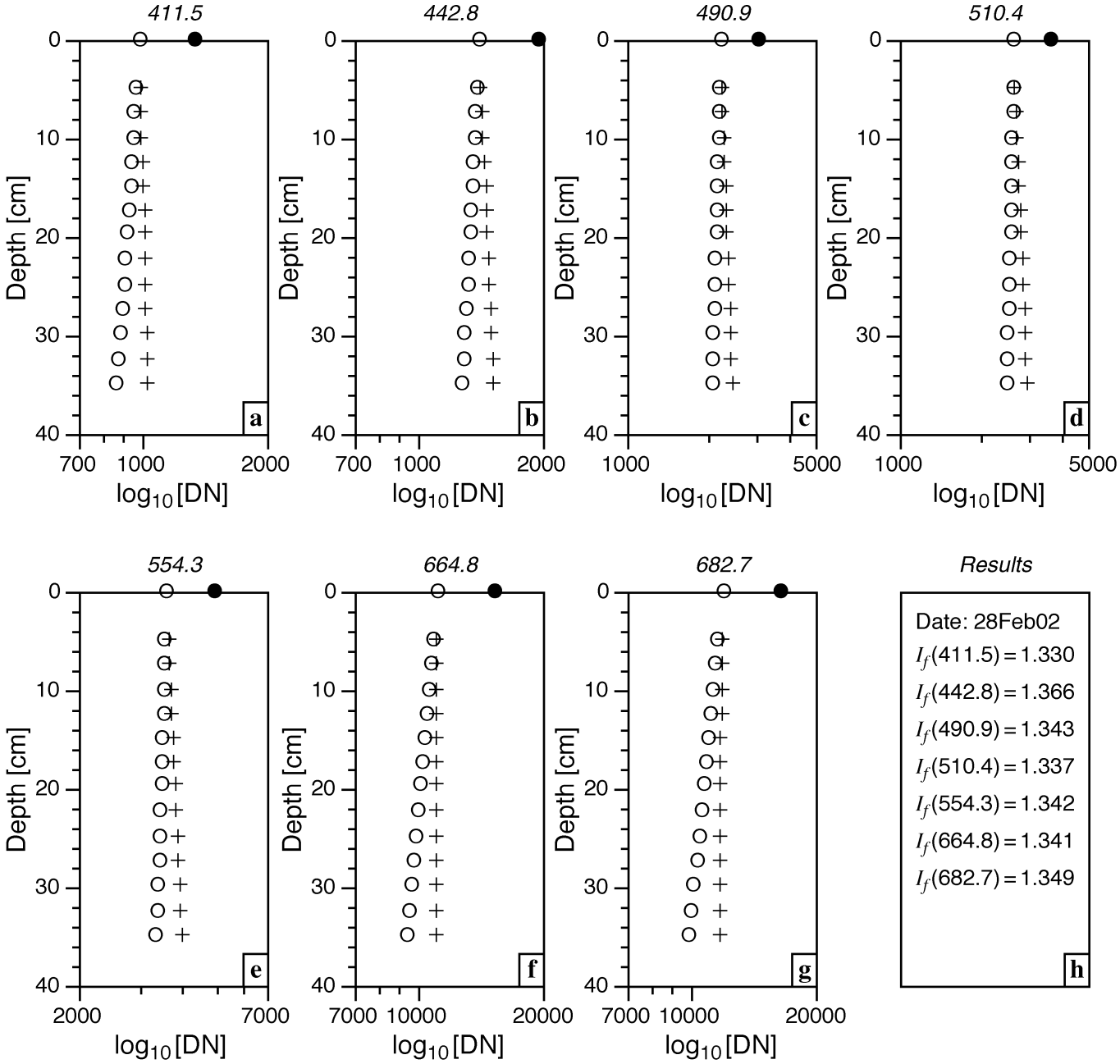

Fig. 6. An example of the plotted measurements for computing immersion factors at different wavelengths: **a)** 411.5 nm, **b)** 442.8 nm, **c)** 490.9 nm, **d)** 510.4 nm, **e)** 554.3 nm, **f)** 664.8 nm, and **g)** 682.7 nm. The x-axis is the net voltage (signal minus dark, signal minus ambient, or signal minus background, depending on the experimental procedures and processing options) measured at each channel and expressed as a digital number (DN). The crosses indicate the actual measurements at different water depths, and the open circles are the corresponding data corrected for geometric effects through the $G(z, \lambda)$ term. The solid circle at zero depth indicates the in-air measurement to be divided by the subsurface extrapolated value (open circle at zero depth). The resulting final $I_f(\lambda)$ values are given in panel **h**.

from the least-squares fit of the logarithm of in-water irradiance data corrected by the measurements perturbations induced by the finite distance between source and collector, i.e., $\ln\left[E(z,\lambda)/G(z,\lambda)\right]$. The correction factor for irradiance data taken at water depth z with a point source at distance d from the collector, $G(z,\lambda)$, is given by (Petzold and Austin 1988):

$$G(z,\lambda) \;=\; \left[1 \;-\; \frac{z}{d}\left(1 \;-\; \frac{1}{n_w(\lambda)}\right)\right]^{-2}. \qquad (4)$$

The spectral values of $n_w(\lambda)$ are user selectable. Two formulations are included in the module to compute $n_w(\lambda)$ in the spectral range of 400–700 nm, based on the salinity of the water. For pure water and pure seawater (salinities of 0 and 35 PSU, respectively) at a temperature of 20°C:

$$n_w(\lambda) \;=\; 1.31891 \;+\; \frac{6.31446}{\lambda - 139.596} \qquad (5)$$

and

$$n_w(\lambda) \;=\; 1.32483 \;+\; \frac{6.53318}{\lambda - 139.589}, \qquad (6)$$

respectively (λ is in units of nanometers). The coefficients in (5) and (6) were obtained by fitting tabulated data from Austin and Halikas (1976) with the least-squares method using the quasi-Newton minimization technique (Press et al. 1992). Equivalent equations were already published by Petzold and Austin (1988) for pure water at a temperature of 22°C, and by Mueller and Austin (1995) for pure seawater at a temperature of 16°C.

5.4 DATA PRESENTATION

Figure 6 shows the graphic output produced by the processing module. Individual plots are shown for each center wavelength of the radiometer, and it permits identification of depth-specific or wavelength-specific data that is affected by measurement perturbations. The computed $I_f(\lambda)$ values are presented on the bottom right corner of the figure.

In addition to the graphic output, a log file is created to permanently store intermediate results from the different processing steps. Particularly relevant are the average values computed for each data file at each wavelength, and the related standard deviations, $\sigma(\lambda)$. A high $\sigma(\lambda)$ value suggests changes in the measurement conditions during data collection (i.e., due to a disturbance of the water surface, the presence of large particles moving over the collectors, etc.).

Other relevant quantities stored in the file log, aside from the specific values used for $I_f(\lambda)$ computation, are the diffuse attenuation coefficient, $K(\lambda)$, values. The latter are the negative slopes of the linear regressions as a function of water depth for the in-water data corrected with the $G(z,\lambda)$ factor. Significant changes in $K(\lambda)$ between successive measurement sequences suggest changes in the water quality or in the optical and mechanical setup of the system.

5.5 SUMMARY

The calibration module included in the JRC Data Processing System was developed primarily to ensure the radiometric calibration of the Satlantic 200- and 500-series of light sensors. Specifically, the module supports the processing of data collected to compute the immersion factor of in-water radiometers. The formulation used follows the basic protocol presented by Mueller and Austin (1995). A GUI implemented in the processing code, provides support for the selection of the source-to-collector distance, the refractive index of water, removing bias voltages using dark or background data, and enabling data normalization using source data collected with a monitoring sensor.

Chapter 6

Cosine Response Measurements

Giuseppe Zibordi
JRC/IES/Inland and Marine Waters Unit
Ispra, Italy

Stanford B. Hooker
NASA/Goddard Space Flight Center
Greenbelt, Maryland

James L. Mueller
SDSU/Center for Hydro-Optics and Remote Sensing
San Diego, California

Scott McLean
Gordana Lazin
Satlantic, Inc.
Halifax, Canada

Abstract

In addition to the immersion factor characterizations, the cosine response was measured for one irradiance sensor at CHORS and Satlantic (motivated by some preliminary measurements at the JRC). The angular response of an OCI-200 in-water radiometer was characterized by CHORS and by Satlantic using a similar methodology, although the former relied on a point source with a horizontal rotation of the sensor, and the latter relied on a collimated source and a vertical rotation. Results from the analysis of the data from Satlantic show deviations from the ideal cosine response for most of the collectors within, or very close to, the limits suggested by the SeaWiFS Ocean Optics Protocols (i.e., 2% between 0–65° and 10% above 65°). Results obtained from the analysis of the CHORS data show deviations from the ideal cosine response within the suggested limits for the OCI-200 central collector, but consistently higher deviations for the six collectors symmetrically located around the centermost one. The latter result is primarily explained by the use of different sources at the two laboratories (i.e., a lamp at CHORS and a lamp plus a collimator at Satlantic).

6.1 INTRODUCTION

The calibration of irradiance sensors takes place in air with light arriving normal to the plane of the cosine collector faceplate. To properly measure all irradiance arriving at the collector plane, the response should follow a cosine function, such that

$$E_\theta \;=\; E_0 \cos\theta, \tag{7}$$

where E_θ is the measured irradiance in response to the light flux arriving at angle θ with respect to the normal of the collector plane, and E_0 is the measured irradiance the same light flux would produce if it were measured normal to the collector plane. Irradiance sensors have a field of view that extends over the hemisphere normal to the sensor faceplate, which is usually separated into two 90° halves, i.e., during a characterization, $-90° < \theta < +90°$.

If (7) is satisfied, an on-axis calibration can be used, and the device will correctly measure the irradiance arriving at the collector plane (regardless of the directional origin of the light). Of course, for an in-water sensor to correctly measure irradiance, there is the added requirement that the immersion factor must be correctly characterized. For in-water irradiance sensors, which were the only ones considered in SIRREX-8, the cosine response must be made with the radiometer under water.

6.2 PRELIMINARY INQUIRIES

A continuing philosophy of the entire SIRREX activity has been to incrementally investigate the sources of uncertainty in radiometric calibrations and measurements. The primary reason for this approach has been the difficulty of assembling the needed resources (personnel, equipment,

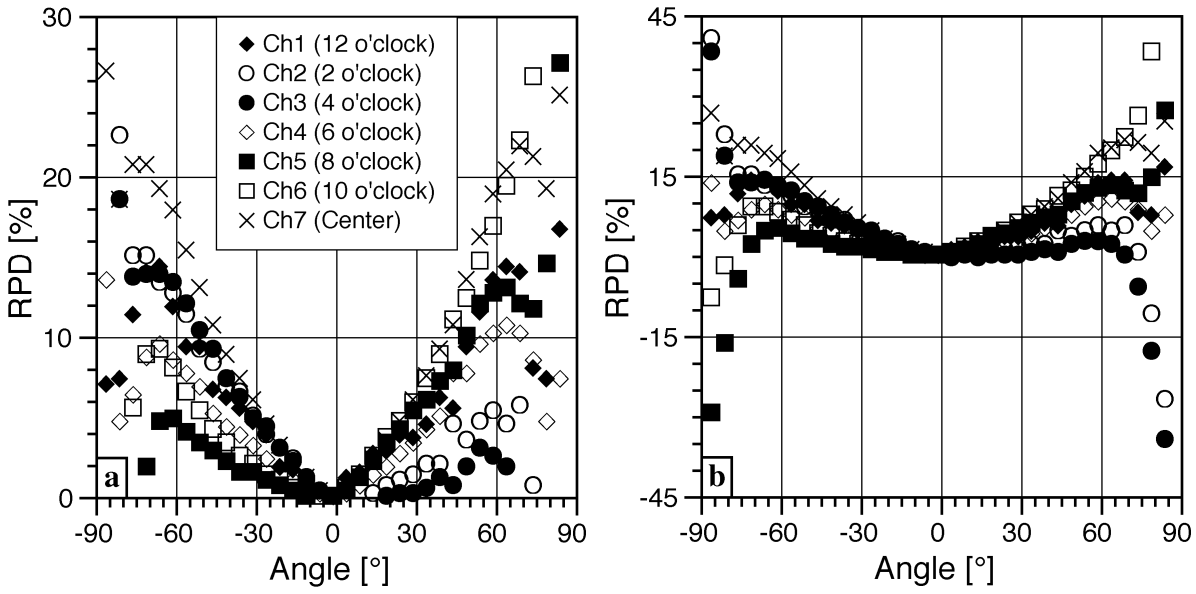

Fig. 7. The relative percent difference (RPD) for the in-air cosine response experiment of an in-water OCI-200 sensor: **a)** a magnified plot, and **b)** the full data set. For this experiment, the angular increment was 5° with a maximum angle of ±85°.

laboratory space, etc.) to conduct complete investigations into the myriad sources of uncertainty identified within the original SeaWiFS Ocean Optics Protocols and its subsequent revisions. Determining the cosine response of an in-water sensor is a time-consuming and laborious exercise, and the effort undertaken here is not be considered definitive—it is simply a first step in the process of understanding the uncertainties involved with this type of measurement and more experiments are needed. Although only one radiometer was involved, it was the reference sensor for the immersion factor experiments, so its performance is well documented.

A submerged sensor imposes practical limitations on changing the angular orientation of the source and the sensor, because there are only two ways to get light into a tank: a) through the water surface, or b) through a window in the tank wall. Most facilities capable of making this type of measurement, use a tank with a window in one wall and rotate the sensor with respect to a fixed source placed on-axis to the window.

The importance of proper metrology and the requirement for measuring in-water sensors submerged during cosine response characterizations are shown in Fig. 7. The figure shows the RPD values of the seven channels of an in-water OCI-200 sensor characterized in air. Assuming the sensor pattern in Fig. 1 corresponds to a clock face, the sensor was placed on-axis to the source with channel 1 in the 12 o'clock position, channel 2 in the 2 o'clock position, etc. The sensor was rotated along the axis defined by channels 1, 4, and 7. The RPD values between the E_θ/E_0 ratio and $\cos\theta$ show significant amplitudes and asymmetries (Fig. 7a). The large amplitudes are a result of measuring an in-water sensor in air, and the asymmetries are associated primarily with the off-axis channels. Sensor rotation causes two significant effects on the off-axis channels:

1. As the radiometer is rotated, the distance between the source and the diffusers not aligned with the rotational axis changes; and
2. At large viewing angles ($|\theta| \rightarrow 90°$) the diffusers can produce reflection and shading effects on each other (Fig. 7b).

6.3 COSINE RESPONSE

Measurements for characterizing the angular response of the OCI-200 in-water irradiance collectors, were carried out at CHORS and Satlantic using the methodology presented in Mueller and Austin (1995), which is in agreement with the basic principles given in Tyler and Smith (1970). Measurements were taken with the radiometer immersed in a tank of water and installed on a rotational system enabling pointing at a source with different angles with respect to the source–radiometer axis. The source, placed outside the tank and aligned with respect to the center of the front plate of the radiometer, was used to illuminate the collectors through a quartz window on a wall of the tank. A circular baffle between the tank and the source was used to reduce the area illuminated on the radiometer front plate and, thus, to minimize the scattering of light in the water.

Measurements were taken at a number of angles, θ, between the direction of the incident light and the direction

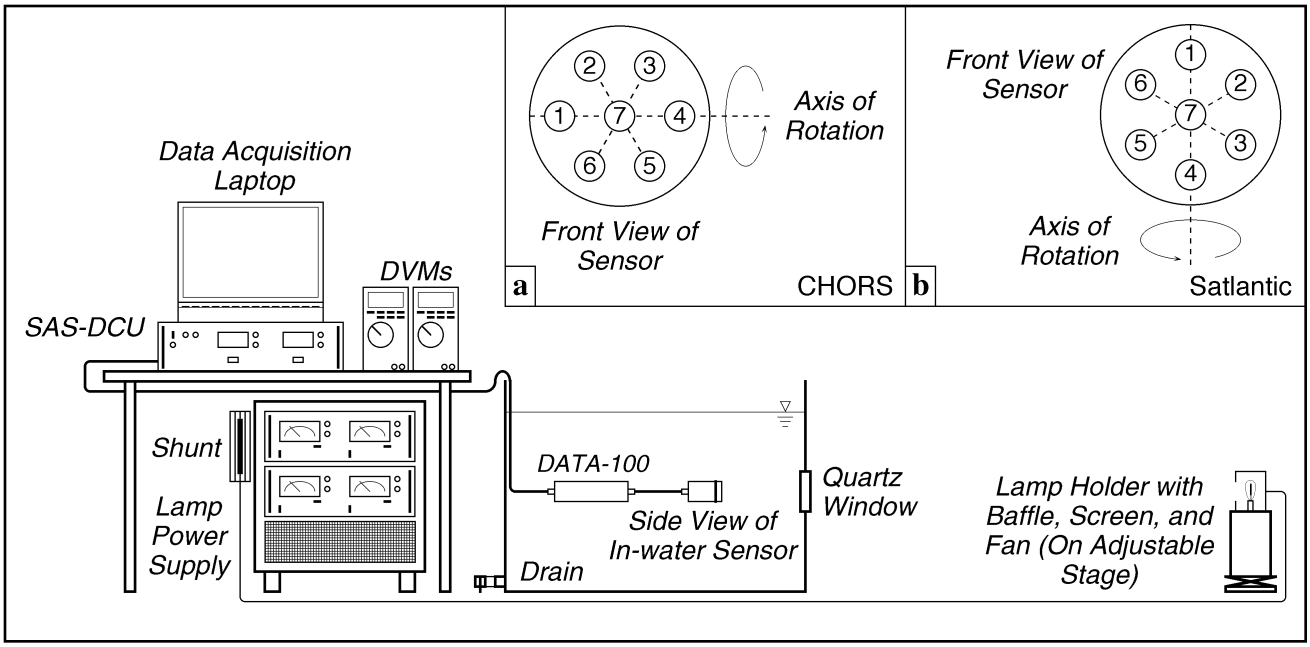

Fig. 8. A generalized schematic of the apparatus used to measure the cosine response of an OCI-200 sensor. The inset panel shows the difference in axis rotation used at **a)** CHORS and **b)** Satlantic. The other primary differences between the two methods were CHORS used a point source (shown) and tap water, whereas Satlantic used a lamp with a collimator (not shown) and seawater. For simplicity and clarity, the mechanical apparatus used to rotate the sensor about the rotation axis is not shown.

perpendicular to the collector horizontal plane. The deviation from the ideal cosine response, ε_θ, was computed as a percentage through

$$\varepsilon_\theta \;=\; 100\left[\frac{V(\theta)}{V(0)}cos\theta \;-\; 1\right], \tag{8}$$

where $V(\theta)$ is the measurement taken at angle θ, and $V(0)$ is the measurement taken at $\theta = 0$. Replicate measurements were taken at different azimuth planes ϕ (e.g., ϕ and $\phi - \pi$) for the same series of angles θ between 0–90°, to minimize measurement uncertainties.

Because the OCI-200 sensor design uses multiple apertures (Fig. 1), repeated measurement sequences were required for the characterization of each collector to ensure respect of the basic requirement of constant distance between the collector and the source at varying angles, θ. A reduction in the number of measurements was obtained by taking simultaneous measurements for groups of three collectors by choosing the rotation axis of the radiometer (i.e., the axis tangent to the front face of the radiometer and laying on the plane identifying the angle θ) coincident with the symmetry axis of three of the seven collectors (Fig. 8). This solution ensured keeping constant the collector–source distance at different angles θ for the three collectors aligned with respect to the rotational axis.

Measurements were performed at CHORS and Satlantic for the three different rows of triplicate collectors (resulting in three characterizations of the central collector). For each group of aligned collectors, the radiometer rotation (i.e., from 0° up to 90°, and then from 0° down to −90°) was made with incremental angles of 5° from 0° up to 75°, and 2.5° above 75° at CHORS, and with incremental angles of 1° at Satlantic. At CHORS, the radiometer rotation was made manually, while at Satlantic it was made automatically using a computer-controlled precision rotator. The long time required for characterizing a sensor restricted the analysis to only one radiometer. The major elements characterizing the measurement procedures applied at CHORS and Satlantic are summarized in Table 11.

Table 11. The major elements for the cosine response measurements at CHORS and Satlantic.

Parameter	*CHORS*	*Satlantic*
Light Source	Lamp	Lamp†
Source–Tank Dist. [m]	1.42	0.20
Sensor–Tank Dist. [m]	0.33	1.00
Source–Sensor Dist. [m]	1.75	1.20
Angular Resolution [°]	5.0‡	1.0
Sampling Period [min]	2.0	1.0
Rotational Axis	Horizontal	Vertical
Water Type	Tap Water	Seawater

†With collimator. ‡2.5° after $\theta = 75°$.

The most important element that differentiated the measurements at the two laboratories was the use of different sources: a lamp with a small filament at CHORS,

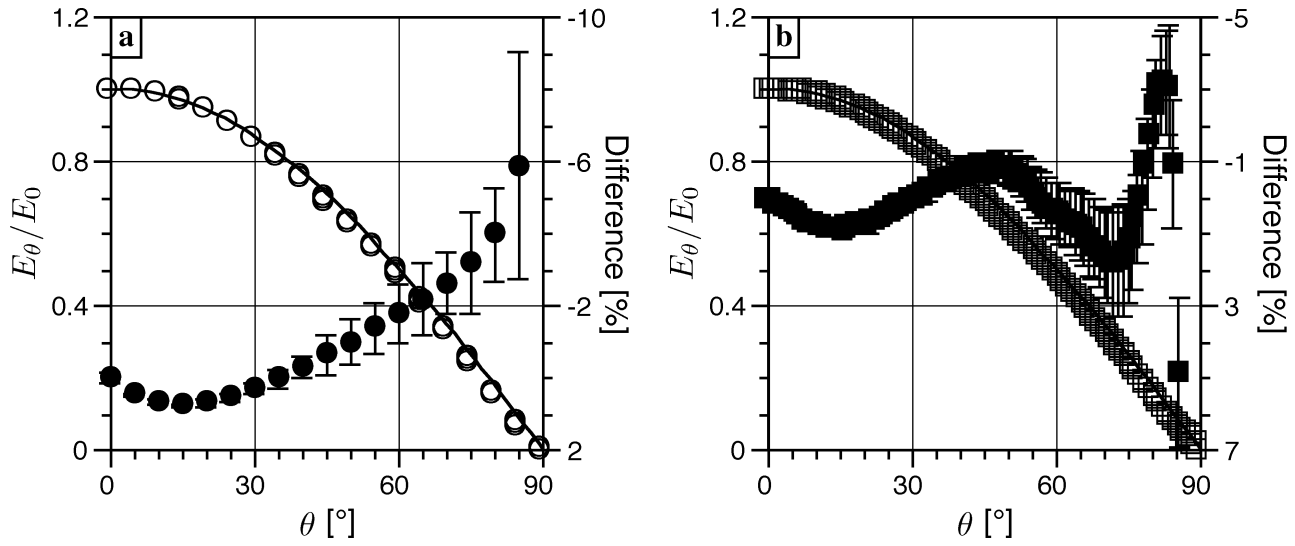

Fig. 9. The experimental angular response (open symbols) and ideal cosine response (solid line), for the OCI-200 (S/N 130) collector at 683 nm: **a)** CHORS (circles), and **b)** Satlantic (squares). Experimental points are actual measurements performed at different azimuth angles. The right axis shows the local percent difference at various θ angles (solid symbols). The error bars indicate the standard deviation in the local percent difference, ε_θ, due to differences in measurements performed in the different azimuthal planes.

and a lamp with a collimator at Satlantic. Other relevant differences were a) the use of tap water at CHORS and filtered seawater at Satlantic, and b) the larger sensor-to-tank distance at Satlantic, which increases the importance of water purity.

Figure 9 displays the results from measurements performed at CHORS and Satlantic for the central collector (i.e., the 683 nm center wavelength) of the E_u sensor (S/N 130). The open symbols show the measurements obtained from the different rotational axes related to different azimuths. Although the results show a deviation from the ideal cosine response of the angular response of the collector for both of the methods, the deviations are well within the requirements defined by the SeaWiFS Ocean Optics Protocols (i.e., 2% between 0–65°, and within 10% above 65°).

The analysis of measurements for the external ring of collectors showed conflicting results. Measurements from Satlantic show deviations from cosine response generally within the SeaWiFS specifications, while measurements from CHORS show generally larger values. A less accurate alignment, added to the use of an uncollimated source at CHORS may somehow explain the former differences.

6.4 SUMMARY

The analysis of the angular response of the collectors for an OCI-200 in-water radiometer was carried out using measurements performed at CHORS and at Satlantic. The results show deviations from the ideal cosine response within the uncertainties required by the SeaWiFS Ocean Optics Protocols for the central collector. Results for the ring of collectors located around the central one show diverging values. Satlantic data values are generally in agreement with the SeaWiFS protocols, whereas the CHORS values are slightly higher. Differences may be justified by the different light sources (a lamp for CHORS, and a lamp plus collimator for Satlantic).

Chapter 7

SIRREX-8 Results, Discussion, and Conclusions

Giuseppe Zibordi
Davide D'Alimonte
JRC/IES/Inland and Marine Waters
Ispra, Italy

Stanford B. Hooker
NASA/Goddard Space Flight Center
Greenbelt, Maryland

James L. Mueller
SDSU/Center for Hydro-Optics and Remote Sensing
San Diego, California

Scott McLean
Gordana Lazin
Satlantic, Inc.
Halifax, Canada

Abstract

The SIRREX-8 experiment for comparing immersion factors involved nine OCI-200 sensors which were all characterized at three different facilities—CHORS, JRC, and Satlantic—using similar laboratory protocols. One of the radiometers, E_u S/N 130, was selected as a so-called *reference* sensor and was measured more frequently than the other eight. The analysis of the SIRREX-8 data showed intralaboratory measurement uncertainties, evaluated through multiple characterizations of the reference radiometer and defined by two standard deviations, ranging from 0.28% for Satlantic, and up to 0.49% and 0.60% for JRC and CHORS, respectively. Interlaboratory uncertainties, evaluated with data from the nine common radiometers, showed average UPDs lower than ±0.6%. The analysis of $I_f(\lambda)$ variability across radiometers of the same series showed average values of approximately 2%, with maximum values of up to 5%, for all three laboratories. Typical $I_f(\lambda)$ values for the OCI-200 series of radiometers were produced with $I_f(\lambda)$ data from measurements taken from the three laboratories.

7.1 INTRODUCTION

The data collected at the three laboratories involved in the SIRREX-8 immersion coefficient intercomparison experiment were analyzed (after quality assurance) to investigate the following:

1. Intralaboratory uncertainties derived from the multiple measurements of the reference radiometer, and
2. Interlaboratory uncertainties derived from the common set of nine radiometers.

Additional objectives of the data analysis were: a) determining the average immersion factors; b) quantifying the variability across the OCI-200 series of radiometers (widely used in ocean color calibration and validation activities); and c) proposing a set of so-called *typical* spectral values for the considered series of radiometers.

7.2 THE DATA SET

The SIRREX-8 data set included the measurements made at CHORS, JRC, and Satlantic for nine OCI-200 radiometers. The methods used at each laboratory followed the protocol described in Mueller and Austin (1995) for the characterization of immersion factors, although there were differences between the published and practiced procedures. Table 12 presents the number of measurement sequences included in the data set. Filtering of measurement sequences affected by perturbations, like poor water quality or radiometer-to-source misalignment, was implemented in near-real time just after each measurement sequence by processing the data with the code described in Chapt. 5. One quality-assured measurement sequence per instrument per laboratory was considered acceptable for comparing data among the three different laboratories.

Table 12. The quality assured and the total number (in parentheses) of measurement sequences carried out for each OCI-200 radiometer at each laboratory.

Sensor	*CHORS*	*JRC*	*Satlantic*
E_d S/N 015	1 (2)	2 (2)	2 (2)
E_d S/N 040	1 (2)	1 (2)	2 (2)
E_u S/N 048	3 (4)	2 (3)	2 (2)
E_d S/N 050	1 (2)	1 (2)	2 (2)
E_d S/N 071	1 (2)	3 (4)	2 (2)
E_d S/N 097	1 (2)	2 (3)	1 (2)
E_u S/N 098	1 (2)	1 (2)	2 (2)
E_u S/N 109	1 (2)	3 (4)	2 (2)
E_u S/N 130	5 (8)	7 (10)	6 (6)
Total	*15 (26)*	*22 (32)*	*21 (22)*

Some of the CHORS data were affected by the presence of large particles floating on and near the water surface. This perturbation, when not removed, produces a decrease in the transmittance of the air–water interface which induces an increase in the computed $I_f(\lambda)$ values. Measurement sequences from CHORS were assumed to be quality assured after introducing surface skimming (generally made before starting the measurement sequence at each water depth) to the measurement protocol.

A subset of the JRC data were affected by a decrease in water purity. This perturbation produced a decrease in computed $I_f(\lambda)$ values, and was primarily caused by enhanced water scattering. The latter was the result of an increase in suspended particles over time as the water aged. Filtering of the JRC data was carried out using a $K(412)$ threshold of $0.2\,\mathrm{m}^{-1}$. One measurement sequence from Satlantic was probably affected by perturbations in the optical and mechanical set up during its execution.

7.3 DATA ANALYSIS

All quality assured data from the three laboratories were processed using the same processing code to ensure the removal of uncertainties which frequently arise from differing parameter settings and approximations. All data were processed using the processor described in Chapt. 5, but with the application of the irradiance normalization option (i.e., the measurements for computing $I_f(\lambda)$ were normalized with respect to simultaneous irradiance measurements of the light source) to minimize uncertainties caused by changes in the light source during execution of the measurement sequence. The processing of CHORS and JRC data was carried out using the refractive index of pure water (5), whereas Satlantic data were processed using the refractive index of pure seawater (6).

The intercomparison among $I_f(\lambda)$ values produced with measurement sequences from the three laboratories, was made using primarily two partitions of the total data set: a) the data from the E_u S/N 130 reference radiometer, and b) the data from all nine common radiometers. These two approaches permit two different inquiries:

1. The data from the reference sensor, besides ensuring intercomparability among the different laboratories, allows a quantification of the reproducibility of the measurements (in fact, for all laboratories the number of measurement sequences for E_u S/N 130 was the largest); and
2. The data from the common sensors, besides assessing intercomparability among the different laboratories, permits an analysis of the variability of $I_f(\lambda)$ data across the OCI-200 production spanning the years 1994–1999 (i.e., this accounts for about 10% of the in-water OCI-200 radiometers manufactured in the time period considered).

The results from these data analyses are presented in the following subsections. The data are given as a function of the nominal center wavelength, λ, of the radiometers (recalling that all the considered OCI-200 sensors included in the experiment had identical nominal center wavelengths).

7.3.1 The Reference Data

Table 13 shows the spectral $I_f(\lambda)$ values of the reference E_u S/N 130 radiometer produced with quality assured measurement sequences from the three different laboratories. The analysis, supported by the N independent measurements produced in each laboratory, is presented as a function of λ through the average, minimum, and maximum of the $I_f(\lambda)$ values, $\bar{I}_f(\lambda)$, $\check{I}_f(\lambda)$, and $\hat{I}_f(\lambda)$, respectively. Quantification of measurement uncertainties is given by two times the standard deviation, σ, divided by $\bar{I}_f$ and expressed as a percentage:

$$\xi^{Ri}(\lambda) \;=\; 200\,\frac{\sigma^{Ri}(\lambda)}{\bar{I}_f^{Ri}(\lambda)}, \qquad (9)$$

where, R is used to denote the reference radiometer, and the i index selects the laboratory using C for CHORS, J for JRC, and S for Satlantic (thus, RC, RJ, and RS are used to indicate values for the reference radiometer produced by CHORS, JRC, and Satlantic, respectively).

The $I_f(\lambda)$ analysis for the reference E_u S/N 130 radiometer shows the lowest and highest average values for CHORS and Satlantic, respectively. The uncertainty in measurements shows the lowest values (i.e., the greatest repeatability in measurements) for Satlantic with average ξ^{RS}=0.28%. JRC and CHORS display average ξ^{RJ} and ξ^{RC} values of 0.49% and 0.60%, respectively. Typically, the highest uncertainties are observed at 412 nm for all three laboratories.

In this study, no one laboratory method is assumed to be more correct than another, so an unbiased parameter is needed to compare the various methods. The latter is

Table 13. Summaries of the CHORS, JRC, and Satlantic $I_f(\lambda)$ data analysis results for E_u S/N 130. The number of oberservations involved are 5, 7, and 6, respectively. The $\xi^{Ri}(\lambda)$ values are in units of percent.

λ	*CHORS*				*JRC*				*Satlantic*			
[nm]	$\check{I}_f^{RC}$	$\bar{I}_f^{RC}$	$\hat{I}_f^{RC}$	ξ^{RC}	$\check{I}_f^{RJ}$	$\bar{I}_f^{RJ}$	$\hat{I}_f^{RJ}$	ξ^{RJ}	$\check{I}_f^{RS}$	$\bar{I}_f^{RS}$	$\hat{I}_f^{RS}$	ξ^{RS}
412	1.327	1.331	1.339	0.71	1.335	1.341	1.349	0.75	1.347	1.351	1.354	0.42
443	1.361	1.367	1.374	0.72	1.372	1.375	1.380	0.45	1.383	1.385	1.386	0.20
490	1.342	1.345	1.351	0.61	1.346	1.349	1.353	0.32	1.352	1.355	1.357	0.27
510	1.332	1.337	1.342	0.59	1.341	1.344	1.347	0.34	1.348	1.351	1.353	0.26
555	1.334	1.338	1.344	0.57	1.342	1.345	1.346	0.24	1.352	1.355	1.360	0.44
665	1.338	1.342	1.347	0.50	1.332	1.343	1.346	0.73	1.355	1.356	1.358	0.17
683	1.345	1.349	1.354	0.48	1.345	1.353	1.358	0.59	1.365	1.366	1.368	0.18
All			*Average*	*0.60*			*Average*	*0.49*			*Average*	*0.28*

accomplished by establishing a truth based on the overall average values computed with the average data from all three laboratories:

$$\bar{I}_f^{RA}(\lambda) \;=\; \frac{\bar{I}_f^{RC}(\lambda) \;+\; \bar{I}_f^{RJ}(\lambda) \;+\; \bar{I}_f^{RS}(\lambda)}{3}, \qquad (10)$$

where the A superscript is used to denote all contributions (i.e., all radiometers). Uncertainties in $\bar{I}_f^{RA}(\lambda)$ are quantified using ξ^{RA} following the formulation given in (9).

The UPD values are computed using (10) and the spectral average data from each laboratory:

$$\psi^{Ri}(\lambda) \;=\; 200\,\frac{\bar{I}_f^{Ri}(\lambda) \;-\; \bar{I}_f^{RA}(\lambda)}{\bar{I}_f^{Ri}(\lambda) \;+\; \bar{I}_f^{RA}(\lambda)}, \qquad (11)$$

where, as in (9), the i index selects the laboratory. UPD values for CHORS, JRC, and Satlantic data are specified by $\psi^{RC}(\lambda)$, $\psi^{RJ}(\lambda)$, and $\psi^{RS}(\lambda)$, respectively. The laboratory intercomparison for the E_u S/N 130 data is presented in Table 14.

Table 14. A summary of the interlaboratory comparison of $\bar{I}_f(\lambda)$ data for E_u S/N 130.

λ	$\bar{I}_f^{RA}$	ξ^{RA}	ψ^{RC}	ψ^{RJ}	ψ^{RS}
[nm]		[%]	[%]	[%]	[%]
412	1.341	1.47	−0.75	0.03	0.72
443	1.376	1.27	−0.62	−0.04	0.65
490	1.350	0.73	−0.36	−0.02	0.38
510	1.344	1.06	−0.53	0.00	0.53
555	1.346	1.21	−0.55	−0.09	0.64
665	1.347	1.16	−0.39	−0.28	0.67
683	1.356	1.33	−0.51	−0.25	0.75
All	*Average*	*1.18*	*−0.53*	*−0.09*	*0.62*

Laboratory intercomparisons, based on the E_u S/N 130 $I_f(\lambda)$ data, show average uncertainties, $\xi^{RA}(\lambda)$, ranging from 0.73% at 490 nm, up to 1.47% at 412 nm, with an average value of 1.18%. The UPDs between average values from each laboratory, $\bar{I}_f^{Ri}(\lambda)$, and the average of data from all three laboratories, $\bar{I}_f^{RA}(\lambda)$, show the lowest values for JRC with $\psi^{RJ}(\lambda)$ ranging from −0.25 to 0.03% with an average of −0.09%. CHORS and Satlantic show UPDs similar in magnitude but with opposite signs. Specifically, CHORS displays $\psi^{RC}(\lambda)$ values ranging from −0.75 to −0.36% with an average of −0.59%. Satlantic $\psi^{RS}(\lambda)$ values range from 0.38 to 0.75% with an average of 0.62%.

7.3.2 The Common Data

Table 15 shows the statistical $I_f(\lambda)$ values produced for the nine common radiometers. When multiple $I_f(\lambda)$ measurements were available for a specific radiometer, the average was used in the analysis. The superscripts AC, AJ, and AS are used to indicate average values for all nine radiometers from CHORS, JRC, and Satlantic, respectively.

The analysis of $I_f(\lambda)$ data for the nine OCI-200 radiometers, confirms the lowest and highest average values for CHORS and Satlantic, respectively, as already observed with the E_u S/N 130 data (Sect. 7.3.1). Variability in $I_f(\lambda)$ values across the different radiometers was quantified with the $\xi^{AC}(\lambda)$, $\xi^{AJ}(\lambda)$, and $\xi^{AS}(\lambda)$ variables, which show very similar average values (i.e., ranging from 2.2–2.3%). Differences between the laboratories are spectrally pronounced, and all three laboratories display high variability in $I_f(490)$ and $I_f(665)$, with values of 3% and 5%, respectively. The lowest variability in the $I_f(\lambda)$ values is observed at 510 nm, with $\xi^{Ai}(\lambda)$ values at each laboratory generally close to, or less than, 1%.

The interlaboratory comparison for the $I_f(\lambda)$ data from all nine OCI-200 radiometers follows from what was developed for the E_u S/N 130 reference data. The UPD is computed between the average data from each laboratory $\left[\text{i.e., } \bar{I}_f^{AC}(\lambda),\ \bar{I}_f^{AJ}(\lambda), \text{ and } \bar{I}_f^{AS}(\lambda)\right]$ and the overall average values $\bar{I}_f^{AA}(\lambda)$ calculated from the average data from the three laboratories

$$\bar{I}_f^{AA}(\lambda) \;=\; \frac{\bar{I}_f^{AC}(\lambda) \;+\; \bar{I}_f^{AJ}(\lambda) \;+\; \bar{I}_f^{AS}(\lambda)}{3}. \qquad (12)$$

The $\xi^{AA}(\lambda)$ parameter is used to quantify uncertainties in the $\bar{I}_f^{AA}(\lambda)$ values. UPD values for the CHORS, JRC,

Table 15. Summaries of the CHORS, JRC, and Satlantic $I_f(\lambda)$ data analysis results for all nine OCI-200 radiometers. The $\xi^{Ai}(\lambda)$ values are in units of percent.

λ	*CHORS*				*JRC*				*Satlantic*			
[nm]	$\check{I}_f^{AC}$	$\bar{I}_f^{AC}$	$\hat{I}_f^{AC}$	ξ^{AC}	$\check{I}_f^{AJ}$	$\bar{I}_f^{AJ}$	$\hat{I}_f^{AJ}$	ξ^{AJ}	$\check{I}_f^{AS}$	$\bar{I}_f^{AS}$	$\hat{I}_f^{AS}$	ξ^{AS}
412	1.331	1.345	1.364	1.78	1.335	1.350	1.370	1.69	1.350	1.362	1.380	1.48
443	1.359	1.373	1.387	1.20	1.367	1.379	1.396	1.30	1.378	1.390	1.401	1.23
490	1.337	1.353	1.402	2.97	1.345	1.359	1.412	3.02	1.354	1.366	1.411	2.57
510	1.327	1.337	1.345	1.04	1.332	1.343	1.350	0.74	1.340	1.353	1.364	0.92
555	1.338	1.355	1.374	1.68	1.345	1.360	1.366	0.89	1.355	1.373	1.391	1.48
665	1.275	1.350	1.389	4.95	1.266	1.351	1.400	5.50	1.282	1.363	1.403	5.12
683	1.349	1.370	1.405	2.47	1.353	1.369	1.408	2.45	1.366	1.382	1.424	2.57
All			*Average*	*2.30*			*Average*	*2.23*			*Average*	*2.20*

and Satlantic data with respect to their average values are specified by $\psi^{AC}(\lambda)$, $\psi^{AJ}(\lambda)$, and $\psi^{AS}(\lambda)$, respectively, and are presented in Table 16.

Table 16. A summary of the interlaboratory comparison of $\bar{I}_f(\lambda)$ data for the nine common OCI-200 sensors.

λ [nm]	$\bar{I}_f^{AA}$	ξ^{AA} [%]	ψ^{AC} [%]	ψ^{AJ} [%]	ψ^{AS} [%]
412	1.352	1.23	−0.52	−0.16	0.68
443	1.381	1.22	−0.54	−0.13	0.66
490	1.359	0.94	−0.45	−0.05	0.49
510	1.344	1.24	−0.55	−0.12	0.66
555	1.363	1.37	−0.54	−0.23	0.77
665	1.355	1.08	−0.36	−0.26	0.62
683	1.374	1.07	−0.30	−0.31	0.61
All	*Average*	*1.16*	*−0.47*	*−0.18*	*0.64*

Laboratory intercomparisons, based on $I_f(\lambda)$ data from all nine OCI-200 radiometers, show an average uncertainty $\xi^{AA}(\lambda)$ of 1.16% displaying the highest values at 555 nm (1.37%) and the lowest at 490 nm (0.94%). The UPD values between average $I_f(\lambda)$ values for all radiometers from each laboratory and the average of data from all three laboratories, $\bar{I}_f^{AA}(\lambda)$, show the lowest values for JRC ranging from −0.31 to 0.05%, with an average of −0.18%. CHORS displays values of $\psi^{AC}(\lambda)$ ranging from −0.55 to −0.30%, with an average of −0.47%. Satlantic displays values of $\psi^{RS}(\lambda)$ ranging from 0.49–0.77%, with an average of 0.64%. All the former results confirm the interlaboratory comparison results produced with the reference E_u S/N 130 $I_f(\lambda)$ data given in Table 14.

7.4 CONCLUSIONS

Values of $I_f(\lambda)$ computed from the Satlantic measurements show the highest repeatability (0.28% defined by two standard deviations). This result can probably be explained with a good alignment procedure and a high stability of the water used (filtered seawater, occasionally chlorinated, and aged for many months). The relatively higher variability in $I_f(\lambda)$ values from CHORS and JRC (0.60 and 0.49%, respectively) can be attributed to different sources of uncertainty. For the CHORS data, it can be justified by slight differences in the alignment of the radiometers with respect to the source (made visually) and by changes over time in the quality of the water (which was taken directly from the tap). For the JRC data, the optical alignment was excellent (made with a laser), so it can only be attributed to changes in water quality over time (caused by dust particles falling onto the water surface and the release of particles from the pump, tanks, and hoses).

The systematic differences in $I_f(\lambda)$ values, seen in the E_u S/N 130 results and confirmed by the analysis of all nine OCI-200 sensors, can be explained by differences in the measurement procedures and the quality and type of water available at the three laboratories. The explanation for differences has focused on three phenomena:

1. The presence of scattering material in the water which produce an underestimate in $I_f(\lambda)$ values,
2. The presence of particles or slicks at the surface which produce an overestimate in $I_f(\lambda)$ values, and
3. The use of different types of water (tap water and seawater), characterized by slightly different refractive indexes, which can bias the retrieved $I_f(\lambda)$.

The analysis of particulate absorption coefficients from water samples from the three laboratories show the highest values for the CHORS water. On a first approximation, the particulate absorption coefficients can be related to the highest concentration of particles in the water, and consequently, to the highest scattering. The use of soap to remove surface particles by Satlantic (as an efficient alternative to the surface skimming used at CHORS and JRC) might produce surface slicks, which would render the use of the transmission factor for an ideal Fresnel water surface, $T_s(\lambda)$ (3), inaccurate. Finally, the use of tap water versus seawater (the former characterized by a slightly lower refractive index) can introduce a negative bias in the CHORS and JRC immersion factors. These observations

support the systematically lower $I_f(\lambda)$ values determined at CHORS (−0.47%) and the systematically higher $I_f(\lambda)$ values determined at Satlantic (+0.64%), assuming the average is the correct value of the immersion factor.

Typical immersion coefficients for the OCI-200 series of sensors were produced using average values computed with the data collected from all three laboratories. The CHORS and JRC $I_f(\lambda)$ values used for the computations were increased by 0.5% to provide an approximate correction for the use of tap water in the laboratory measurements rather than seawater (the correction is assumed to be of the same order of the differences between refractive indexes of pure water and pure seawater). This approach is considered a viable solution, because the UPD values between the overall averages and the specific laboratory results are less than ±0.6%, while the spectral uncertainties due to differences across radiometers of the same series are on average larger than ±2%.

Figure 10 presents the spectral JRC $I_f(\lambda)$ values for the nine OCI-200 radiometers included in the experiment. The graphs clearly show outliers at 490 and at 665 nm from E_d S/N 015. Other radiometers exhibiting significant differences from the average are E_u S/N 048 and E_d S/N 050 at 665 nm, and E_d S/N 040 at 683 nm. All these radiometers are the oldest among those included in the experiment. The outliers do not show any consistent spectral trend, so their values can only be justified by damaged collectors (not observed during a visual inspection) or by differences produced in the manufacturing process of the collectors.

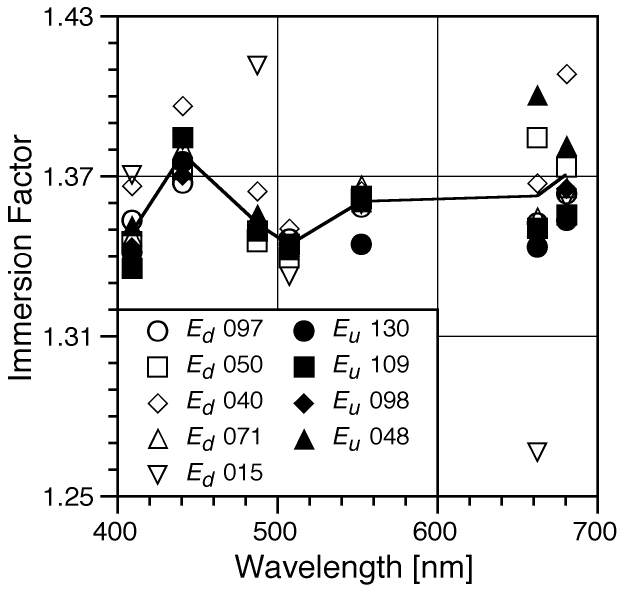

Fig. 10. $I_f(\lambda)$ data (computed from the JRC measurements) for the nine common OCI-200 radiometers. The solid line is the average of all the sensors except E_d S/N 015.

If the data from E_d S/N 015 are ignored, the uncertainty defined by 2σ for the JRC data set goes from 3.02% and 5.50%, to 0.86% and 2.96%, at 490 nm and 665 nm, respectively. Typical values, computed excluding E_d S/N 015, are proposed for the OCI-200 series of radiometers and displayed in Fig. 11 together with $I_f(\lambda)$ values supplied by Satlantic (based on experiments performed in 1994) for the same series of radiometers. For completeness, the same data are also given in Table 17 together with correction factors for the reprocessing of historical data calibrated with the 1994 Satlantic $I_f(\lambda)$ values. The two sets of typical $I_f(\lambda)$ values (i.e., those produced in this study and those released by Satlantic in 1994) show differences ranging from +12% to −6% at 412 and 683 nm, respectively.

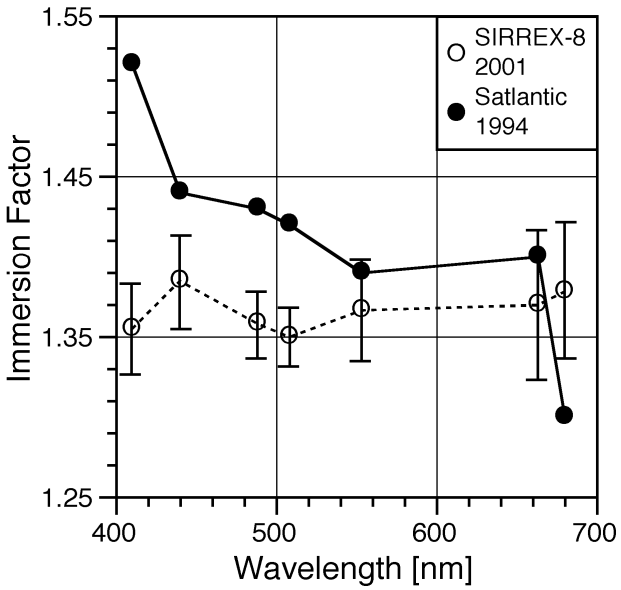

Fig. 11. Typical $I_f(\lambda)$ values from the SIRREX-8 activity (dashed line) versus the 1994 Satlantic values (solid line) for the OCI-200 series of radiometers. The uncertainty bars for the former include both average interlaboratory differences and $I_f(\lambda)$ variability (E_d S/N 015 excluded).

Table 17. Typical $I_f(\lambda)$ values from SIRREX-8 and the 1994 Satlantic characterizations plus related correction factors. The values in parentheses are the estimated maximum uncertainties computed as the sum of the average interlaboratory differences and $I_f(\lambda)$ variability across the OCI-200 radiometers (E_d S/N 015 excluded).

λ [nm]	*SIRREX-8* (2001)	*Satlantic* (1994)	*Correction Factor*
412	1.355 (± 2.1%)	1.52	0.891
443	1.385 (± 2.1%)	1.44	0.962
490	1.358 (± 1.5%)	1.43	0.950
510	1.350 (± 1.4%)	1.42	0.951
555	1.367 (± 2.3%)	1.39	0.983
665	1.370 (± 3.4%)	1.40	0.978
683	1.379 (± 3.1%)	1.30	1.061

The spectral dependence of $I_f(\lambda)$ was discussed in Tyler and Smith (1970) who suggested it was a function of the diffuser absorbance. Tyler and Smith (1970), Petzold and Austin (1988), and Muller (1995), observed an almost linear change of I_f with λ, with some deviation from linearity in the blue part of the spectrum. Such a linear dependence was not observed with the SIRREX-8 $I_f(\lambda)$ measurements for the OCI-200 series of radiometers. A possible explanation for this apparent discrepancy is differences in sensor design. The instruments analyzed by Tyler and Smith (1970), Petzold and Austin (1988), and Mueller (1995) all had a single cosine collector, while the OCI-200 series of radiometers have multiple collectors (one per spectral channel) each designed to have an optimum performance (in terms of scattering and transmittance) at a specific center wavelength.

The observed instrument-to-instrument variability in the spectral $I_f(\lambda)$ values for the OCI-200 series of radiometers (2% on average with maximum values reaching 5%) fully supports—and further highlights—the recommendation of Mueller (1995)† for individual characterizations of the $I_f(\lambda)$ values for each underwater radiometer when accurate absolute radiometric measurements are required.

The SIRREX-8 results suggest the following recommendations should be adopted to increase the accuracy in immersion factor characterizations:

1. Use the purest water possible to reduce the scattering effects of suspended particles (the use of seawater versus tap water, when characterized by the same level of purity, has to be considered a more ideal solution);
2. Use surface skimming to remove floating particles which may change the surface transmittance (the alternative use of soap requires further investigation, because the soap slick which forms at the surface may affect the surface transmittance);
3. Use quality-assurance indices (like the K value) to filter out measurement sequences affected by a decreased quality of water or changes in the optical and mechanical setup; and
4. Use of monitoring devices (i.e., a radiometer or a shunt in series with the lamp) to check the stability of the source during measurement sequences.

† The Mueller (1995) recommendation was the result of a similar, but independent, analysis on a different series of radiometers from a different manufacturer.

Acknowledgments

SIRREX-8 could not have been executed at the high level that was achieved without the competent contributions of the technical staff at the JRC. Many individuals, not immediately associated with the day-to-day execution of the experiments, responded willingly and cheerfully whenever their expertise or assistance was required. The characterization of the OCI-200 radiometers carried out by CHORS and Satlantic, was supported by JRC.

Editorial Note

Chapter 4 of this document is presented *as submitted* with very minor modifications to correct typographical or obvious clerical errors and to maintain the established style of the *SeaWiFS Postlaunch Technical Report Series*.

Appendices

Appendix A

SIRREX-8 Science Team

The SIRREX-8 science team members are presented alphabetically.

Jean-François Berthon
JRC/IES/IMW T.P. 272
I–21020 Ispra (VA)
ITALY
Voice: 39–0–332–789–934
Fax: 39–0–332–789–034
Net: jean-francois.berthon@jrc.it

Davide D'Alimonte
JRC/IES/IMW T.P. 272
I–21020 Ispra (VA)
ITALY
Voice: 39–0–332–785–727
Fax: 39–0–332–789–034
Net: davide.d'alimonte@jrc.it

Stanford Hooker
NASA/GSFC/Code 970.2
Bldg. 28, Room W126
Greenbelt, Maryland 20771
Voice: 301–286–9503
Fax: 301–286–0268
Net: stan@ardbeg.gsfc.nasa.gov

Gordana Lazin
Satlantic, Inc.
Richmond Terminal, Pier 9
3481 North Marginal Road
Halifax, Nova Scotia B3K 5X8
CANADA
Voice: 01–902–492–4780
Fax: 01–902–492–4781
Net: gogo@satlantic.com

Dirk van der Linde
JRC/IES/IMW T.P. 272
I–21020 Ispra (VA)
ITALY
Voice: 39–0–332–785–362
Fax: 39–0–332–789–034
Net: dirk.vanderlinde@jrc.it

Scott McLean
Satlantic, Inc.
Richmond Terminal, Pier 9
3481 North Marginal Road
Halifax, Nova Scotia B3K 5X8
CANADA
Voice: 01–902–492–4780
Fax: 01–902–492–4781
Net: scott@satlantic.com

James Mueller
SDSU/CHORS
6505 Alvardo Road, Suite 206
San Diego, California 92120
Voice: 619–594–2230
Fax: 619–594–8670
Net: jim@chors.sdsu.edu

Giuseppe Zibordi
JRC/IES/IMW T.P. 272
I–21020 Ispra (VA)
ITALY
Voice: 39–0–332–785–902
Fax: 39–0–332–789–034
Net: giuseppe.zibordi@jrc.it

Glossary

CHORS	Center for Hydro-Optics and Remote Sensing
DARR	Data Analysis Round-Robin
DARR-94	The first DARR (1994)
DARR-00	The second DARR (2000)
DATA-100	Not an acronym, but a designator for the Satlantic, Inc., series of power and telemetry units.
DVM	Digital Voltmeter
GSFC	Goddard Space Flight Center
GUI	Graphical User Interface
HP	Hewlett-Packard
IDL	Interactive Data Language
JRC	Joint Research Centre
MVDS	Multichannel Visible Detector System
NASA	National Aeronautics and Space Administration
NIST	National Institute of Standards and Technology
OCI	Ocean Color Irradiance (sensor)
OCI-200	OCI 200-series (sensor)
OCP	Ocean Color Profiler
OCR	Ocean Color Radiance (sensor)
OCR-200	OCR series-200 (analog sensor)
OCR-504	OCR series-504 (four-channel, digital sensor)
OCR-507	OCR series-507 (seven-channel, digital sensor)
PRO-DCU	Not an acronym, but a designator for the Satlantic, Inc., series of 48–76 V deck boxes.
PS	Power Supply

RPD Relative Percent Difference
S/N Serial Number
SAS-DCU Not an acronym, but a designator for the Satlantic, Inc., series of 15 V deck boxes.
SeaWiFS Sea-viewing Wide Field-of-view Sensor
SDY Sequential Day of the Year
SIRREX SeaWiFS Intercalibration Round-Robin Experiment
SIRREX-1 The First SIRREX (July 1992)
SIRREX-3 The Third SIRREX (September 1994)
SIRREX-4 The Fourth SIRREX (May 1995)
SIRREX-6 The Sixth SIRREX (August–December 1997)
SIRREX-7 The Seventh SIRREX (March 1999)
SIRREX-8 The Eighth SIRREX (September–December 2001)
SNR Signal-to-Noise Ratio
SOOP SeaWiFS Ocean Optics Protocols
UPD Unbiased Percent Difference
UPS Uninterruptable Power System

Symbols

A The code used for indicating all the measurements.
C The code used for indicating the CHORS measurements.
$C_c(\lambda)$ The spectral calibration coefficient.
d The distance between the lamp and the diffuser faceplate.
$\bar{D}(\lambda)$ The average bias or dark voltage.
E_0 The measured irradiance the same light flux would produce if it were measured normal to the collector plane.
E_θ The measured irradiance with the incident flux arriving at the angle θ with respect to the collector plane.
$E(\lambda)$ Spectral irradiance.
$E(z,\lambda)$ In-water spectral irradiance.
$E(0^+,\lambda)$ In-air spectral irradiance.
$E_d(0^+,\lambda)$ Above-water total solar irradiance.
$E_d(z,\lambda)$ In-water spectral downward irradiance.
$E_u(z,\lambda)$ In-water spectral upward irradiance.
$G(z,\lambda)$ In-water spectral correction for geometric effects.
$I_f(\lambda)$ The spectral immersion factor.
$\bar{I}_f(\lambda)$ The average spectral immersion factor.
$\check{I}_f(\lambda)$ The minimum spectral immersion factor.
$\hat{I}_f(\lambda)$ The maximum spectral immersion factor.
J The code used for indicating the JRC measurements.
$K(\lambda)$ The spectral diffuse attenuation coefficient.
$n_a(\lambda)$ The refractive index of air.
$n_w(\lambda)$ The refractive index of water.
N_T^C Number of measurement trials performed at CHORS.
N_T^J Number of measurement trials performed at JRC.
N_T^S Number of measurement trials performed at Satlantic.
R The code for indicating the reference radiometer (E_u S/N 130).
S The code used for indicating the Satlantic measurements.
S Salinity.
t Time.
t_i A particular time.
t_0 A reference time (generally chosen to coincide with the start of a measurement sequence).
$T_s(\lambda)$ The spectral transmittance of the water surface to downward irradiance.
$V(\lambda)$ Spectral digitized voltages (in counts).
z The vertical (depth) coordinate, where the depth is the height of water above the cosine collectors.
ε_θ The deviation from the ideal cosine response.
θ The angle with respect to the normal of the collector plane.
λ Wavelength.
$\xi(\lambda)$ Spectral measurement uncertainty.
σ Standard deviation.
$\psi(\lambda)$ The spectral UPD.

References

Austin, R.W., and G. Halikas, 1976: The index of refraction of seawater. *SIO Ref. 76–1*, Vis. Lab., Scripps Institution of Oceanography, La Jolla, California, 64 pp.

D'Alimonte, D., G. Zibordi, and J-F. Berthon, 2001: "The JRC Data Processing System." In: Hooker, S.B., G. Zibordi, J-F. Berthon, D. D'Alimonte, S. Maritorena, S. McLean, and J. Sildam, Results of the Second SeaWiFS Data Analysis Round Robin, March 2000 (DARR-00). *NASA Tech. Memo. 2001–206892, Vol. 15,* S.B. Hooker and E.R. Firestone, Eds., NASA Goddard Space Flight Center, Greenbelt, Maryland, 52–56.

Hooker, S.B., W.E. Esaias, G.C. Feldman, W.W. Gregg, and C.R. McClain, 1992: An Overview of SeaWiFS and Ocean Color. *NASA Tech. Memo. 104566, Vol. 1,* S.B. Hooker and E.R. Firestone, Eds., NASA Goddard Space Flight Center, Greenbelt, Maryland, 24 pp., plus color plates.

——, and ——, 1993: An overview of the SeaWiFS project. *Eos, Trans., Amer. Geophys. Union,* **74,** 241–246.

——, and J. Aiken, 1998: Calibration evaluation and radiometric testing of field radiometers with the SeaWiFS Quality Monitor (SQM). *J. Atmos. Oceanic Technol.,* **15,** 995–1,007.

——, G. Zibordi, J-F. Berthon, D. D'Alimonte, S. Maritorena, S. McLean, and J. Sildam, 2001: Results of the Second SeaWiFS Data Analysis Round Robin, March 2000 (DARR-00). *NASA Tech. Memo. 2001–206892, Vol. 15,* S.B. Hooker and E.R. Firestone, Eds., NASA Goddard Space Flight Center, Greenbelt, Maryland, 71 pp.

——, S. McLean, J. Sherman, M. Small, G. Lazin, G. Zibordi, and J.W. Brown, 2002: The Seventh SeaWiFS Intercalibration Round-Robin Experiment (SIRREX-7), March 1999. *NASA Tech. Memo. 2002–206892, Vol. 17,* S.B. Hooker and E.R. Firestone, Eds., NASA Goddard Space Flight Center, Greenbelt, Maryland, 69 pp.

Johnson, B.C., S.S. Bruce, E.A. Early, J.M. Houston, T.R. O'Brian, A. Thompson, S.B. Hooker, and J.L. Mueller, 1996: The Fourth SeaWiFS Intercalibration Round-Robin Experiment (SIRREX-4), May 1995. *NASA Tech. Memo. 104566, Vol. 37,* S.B. Hooker and E.R. Firestone, Eds., NASA Goddard Space Flight Center, Greenbelt, Maryland, 65 pp.

——, H.W. Yoon, S.S. Bruce, P-S. Shaw, A. Thompson, S.B. Hooker, R.E. Eplee, Jr., R.A. Barnes, S. Maritorena, and J.L. Mueller, 1999: The Fifth SeaWiFS Intercalibration Round-Robin Experiment (SIRREX-5), July 1996. *NASA Tech. Memo. 1999–206892, Vol. 7,* S.B. Hooker and E.R. Firestone, Eds., NASA Goddard Space Flight Center, Greenbelt, Maryland, 75 pp.

Mueller, J.L., 1993: The First SeaWiFS Intercalibration Round-Robin Experiment, SIRREX-1, July 1992. *NASA Tech. Memo. 104566, Vol. 14,* S.B. Hooker and E.R. Firestone, Eds., NASA Goddard Space Flight Center, Greenbelt, Maryland, 60 pp.

——, 1995: "Comparison of Irradiance Immersion Coefficients for Several Marine Environmental Radiometers (MERs)." In: Mueller, J.L., R.S. Fraser, S.F. Biggar, K.J. Thome, P.N. Slater, A.W. Holmes, R.A. Barnes, C.T. Weir, D.A. Siegel, D.W. Menzies, A.F. Michaels, and G. Podesta: Case Studies for SeaWiFS Calibration and Validation, Part 3. *NASA Tech. Memo. 104566, Vol. 27,* S.B. Hooker, E.R. Firestone, and J.G. Acker, Eds., NASA Goddard Space Flight Center, Greenbelt, Maryland, 46 pp.

——, 2000: "Overview of Measurement and Data Analysis Protocols." In: G.S. Fargion and J.L. Mueller, Ocean Optics Protocols for Satellite Ocean Color Sensor Validation, Revision 2. *NASA Tech. Memo. 2000–209966,* NASA Goddard Space Flight Center, Greenbelt, Maryland, 87–97.

——, and R.W. Austin, 1992: Ocean Optics Protocols for SeaWiFS Validation. *NASA Tech. Memo. 104566, Vol. 5,* S.B. Hooker and E.R. Firestone, Eds., NASA Goddard Space Flight Center, Greenbelt, Maryland, 43 pp.

——, B.C. Johnson, C.L. Cromer, J.W. Cooper, J.T. McLean, S.B. Hooker, and T.L. Westphal, 1994: The Second SeaWiFS Intercalibration Round-Robin Experiment, SIRREX-2, June 1993. *NASA Tech. Memo. 104566, Vol. 16,* S.B. Hooker and E.R. Firestone, Eds., NASA Goddard Space Flight Center, Greenbelt, Maryland, 121 pp.

——, and R.W. Austin, 1995: Ocean Optics Protocols for SeaWiFS Validation, Revision 1. *NASA Tech. Memo. 104566, Vol. 25,* S.B. Hooker, E.R. Firestone, and J.G. Acker, Eds., NASA Goddard Space Flight Center, Greenbelt, Maryland, 67 pp.

——, B.C. Johnson, C.L. Cromer, S.B. Hooker, J.T. McLean, and S.F. Biggar, 1996: The Third SeaWiFS Intercalibration Round-Robin Experiment (SIRREX-3), 19–30 September 1994. *NASA Tech. Memo. 104566, Vol. 34,* S.B. Hooker, E.R. Firestone, and J.G. Acker, Eds., NASA Goddard Space Flight Center, Greenbelt, Maryland, 78 pp.

——, C. Pietras, S.B. Hooker, D.K. Clark, A. Morel, R. Frouin, B.G. Mitchell, R.R. Bidigare, C. Trees, J. Werdell, G.S. Fargion, R. Arnone, R.W. Austin, S. Bailey, W. Broenkow, S.W. Brown, K. Carder, C. Davis, J. Dore, M. Feinholz, S. Flora, Z.P. Lee, B. Holben, B.C. Johnson, M. Kahru, D.M. Karl, Y.S. Kim, K.D. Knobelspiesse, C.R. McClain, S. McLean, M. Miller, C.D. Mobley, J. Porter, R.G. Steward, M. Stramska, L. Van Heukelem, K. Voss, J. Wieland, M.A. Yarbrough, and M. Yuen, 2002: Ocean Optics Protocols for Satellite Ocean Color Sensor Validation, Revision 3, Volume 1. *NASA Tech. Memo. 2002–210004/Rev3–Vol1,* J.L. Mueller and G.S. Fargion, Eds., NASA Goddard Space Flight Center, Greenbelt, Maryland, 137 pp.

Petzold, T.J., and R.W. Austin, 1988: Characterization of MER 1032. *Tech. Memo. EN–001–88t*, Vis. Lab., Scripps Institution of Oceanography, La Jolla, California, 56 pp. plus appendices.

Press, W.H., S.A. Tuekolsky, W.T. Vettering, and B.P. Flannery, 1992: *Numerical Recipes in C: The Art of Scientific Computing.* Cambridge University Press, Cambridge, United Kingdom, 994 pp.

Riley, T., and S. Bailey, 1998: The Sixth SeaWiFS/SIMBIOS Intercalibration Round-Robin Experiment (SIRREX-6) August–December 1997. *NASA Tech. Memo. 1998–206878,* NASA Goddard Space Flight Center, Greenbelt, Maryland, 26 pp.

Siegel, D.A., M.C. O'Brien, J.C. Sorensen, D.A. Konnoff, E.A. Brody, J.L. Mueller, C.O. Davis, W.J. Rhea, and S.B. Hooker, 1995: Results of the SeaWiFS Data Analysis Round-Robin (DARR-94), July 1994. *NASA Tech. Memo. 104566, Vol. 26,* S.B. Hooker and E.R. Firestone, Eds., NASA Goddard Space Flight Center, Greenbelt, Maryland, 58 pp.

Tyler, J.E., and R.C. Smith, 1970: *Measurements of Spectral Irradiance Underwater.* Gordon and Breach, New York, 103 pp.

The SeaWiFS Postlaunch Technical Report Series

Vol. 1

Johnson, B.C., J.B. Fowler, and C.L. Cromer, 1998: The SeaWiFS Transfer Radiometer (SXR). *NASA Tech. Memo. 1998–206892, Vol. 1,* S.B. Hooker and E.R. Firestone, Eds., NASA Goddard Space Flight Center, Greenbelt, Maryland, 58 pp.

Vol. 2

Aiken, J., D.G. Cummings, S.W. Gibb, N.W. Rees, R. Woodd-Walker, E.M.S. Woodward, J. Woolfenden, S.B. Hooker, J-F. Berthon, C.D. Dempsey, D.J. Suggett, P. Wood, C. Donlon, N. González-Benítez, I. Huskin, M. Quevedo, R. Barciela-Fernandez, C. de Vargas, and C. McKee, 1998: AMT-5 Cruise Report. *NASA Tech. Memo. 1998–206892, Vol. 2,* S.B. Hooker and E.R. Firestone, Eds., NASA Goddard Space Flight Center, Greenbelt, Maryland, 113 pp.

Vol. 3

Hooker, S.B., G. Zibordi, G. Lazin, and S. McLean, 1999: The SeaBOARR-98 Field Campaign. *NASA Tech. Memo. 1999–206892, Vol. 3,* S.B. Hooker and E.R. Firestone, Eds., NASA Goddard Space Flight Center, Greenbelt, Maryland, 40 pp.

Vol. 4

Johnson, B.C., E.A. Early, R.E. Eplee, Jr., R.A. Barnes, and R.T. Caffrey, 1999: The 1997 Prelaunch Radiometric Calibration of SeaWiFS. *NASA Tech. Memo. 1999–206892, Vol. 4,* S.B. Hooker and E.R. Firestone, Eds., NASA Goddard Space Flight Center, Greenbelt, Maryland, 51 pp.

Vol. 5

Barnes, R.A., R.E. Eplee, Jr., S.F. Biggar, K.J. Thome, E.F. Zalewski, P.N. Slater, and A.W. Holmes 1999: The SeaWiFS Solar Radiation-Based Calibration and the Transfer-to-Orbit Experiment. *NASA Tech. Memo. 1999–206892, Vol. 5,* S.B. Hooker and E.R. Firestone, Eds., NASA Goddard Space Flight Center, 28 pp.

Vol. 6

Firestone, E.R., and S.B. Hooker, 2000: SeaWiFS Postlaunch Technical Report Series Cumulative Index: Volumes 1–5. *NASA Tech. Memo. 2000–206892, Vol. 6,* S.B. Hooker and E.R. Firestone, Eds., NASA Goddard Space Flight Center, Greenbelt, Maryland, 14 pp.

Vol. 7

Johnson, B.C., H.W. Yoon, S.S. Bruce, P-S. Shaw, A. Thompson, S.B. Hooker, R.E. Eplee, Jr., R.A. Barnes, S. Maritorena, and J.L. Mueller, 1999: The Fifth SeaWiFS Intercalibration Round-Robin Experiment (SIRREX-5), July 1996. *NASA Tech. Memo. 1999–206892, Vol. 7,* S.B. Hooker and E.R. Firestone, Eds., NASA Goddard Space Flight Center, 75 pp.

Vol. 8

Hooker, S.B., and G. Lazin, 2000: The SeaBOARR-99 Field Campaign. *NASA Tech. Memo. 2000–206892, Vol. 8,* S.B. Hooker and E.R. Firestone, Eds., NASA Goddard Space Flight Center, 46 pp.

Vol. 9

McClain, C.R., E.J. Ainsworth, R.A. Barnes, R.E. Eplee, Jr., F.S. Patt, W.D. Robinson, M. Wang, and S.W. Bailey, 2000: SeaWiFS Postlaunch Calibration and Validation Analyses, Part 1. *NASA Tech. Memo. 2000–206892, Vol. 9,* S.B. Hooker and E.R. Firestone, Eds., NASA Goddard Space Flight Center, 82 pp.

Vol. 10

McClain, C.R., R.A. Barnes, R.E. Eplee, Jr., B.A. Franz, N.C. Hsu, F.S. Patt, C.M. Pietras, W.D. Robinson, B.D. Schieber, G.M. Schmidt, M. Wang, S.W. Bailey, and P.J. Werdell, 2000: SeaWiFS Postlaunch Calibration and Validation Analyses, Part 2. *NASA Tech. Memo. 2000–206892, Vol. 10,* S.B. Hooker and E.R. Firestone, Eds., NASA Goddard Space Flight Center, 57 pp.

Vol. 11

O'Reilly, J.E., S. Maritorena, M.C. O'Brien, D.A. Siegel, D. Toole, D. Menzies, R.C. Smith, J.L. Mueller, B.G. Mitchell, M. Kahru, F.P. Chavez, P. Strutton, G.F. Cota, S.B. Hooker, C.R. McClain, K.L. Carder, F. Müller-Karger, L. Harding, A. Magnuson, D. Phinney, G.F. Moore, J. Aiken, K.R. Arrigo, R. Letelier, and M. Culver 2000: SeaWiFS Postlaunch Calibration and Validation Analyses, Part 3. *NASA Tech. Memo. 2000–206892, Vol. 11,* S.B. Hooker and E.R. Firestone, Eds., NASA Goddard Space Flight Center, 49 pp.

Vol. 12

Firestone, E.R., and S.B. Hooker, 2000: SeaWiFS Postlaunch Technical Report Series Cumulative Index: Volumes 1–11. *NASA Tech. Memo. 2000–206892, Vol. 12,* S.B. Hooker and E.R. Firestone, Eds., NASA Goddard Space Flight Center, Greenbelt, Maryland, 24 pp.

Vol. 13

Hooker, S.B., G. Zibordi, J-F. Berthon, S.W. Bailey, and C.M. Pietras, 2000: The SeaWiFS Photometer Revision for Incident Surface Measurement (SeaPRISM) Field Commissioning. *NASA Tech. Memo. 2000–206892, Vol. 13,* S.B. Hooker and E.R. Firestone, Eds., NASA Goddard Space Flight Center, Greenbelt, Maryland, 24 pp.

Vol. 14

Hooker, S.B., H. Claustre, J. Ras, L. Van Heukelem, J-F. Berthon, C. Targa, D. van der Linde, R. Barlow, and H. Sessions, 2000: The First SeaWiFS HPLC Analysis Round-Robin Experiment (SeaHARRE-1). *NASA Tech. Memo. 2000–206892, Vol. 14,* S.B. Hooker and E.R. Firestone, Eds., NASA Goddard Space Flight Center, Greenbelt, Maryland, 42 pp.

Vol. 15

Hooker, S.B., G. Zibordi, J-F. Berthon, D. D'Alimonte, S. Maritorena, S. McLean, and J. Sildam, 2001: Results of the Second SeaWiFS Data Analysis Round Robin, March 2000 (DARR-00). *NASA Tech. Memo. 2001–206892, Vol. 15,* S.B. Hooker and E.R. Firestone, Eds., NASA Goddard Space Flight Center, Greenbelt, Maryland, 71 pp.

Vol. 16

Patt, F.S., 2002: Navigation Algorithms for the SeaWiFS Mission. *NASA Tech. Memo. 2002–206892, Vol. 16,* S.B. Hooker and E.R. Firestone, Eds., NASA Goddard Space Flight Center, Greenbelt, Maryland, 17 pp.

Vol. 17

Hooker, S.B., S. McLean, J. Sherman, M. Small, G. Lazin, G. Zibordi, and J.W. Brown, 2002: The Seventh SeaWiFS Intercalibration Round-Robin Experiment (SIRREX-7), March 1999. *NASA Tech. Memo. 2002–206892, Vol. 17,* S.B. Hooker and E.R. Firestone, Eds., NASA Goddard Space Flight Center, Greenbelt, Maryland, 69 pp.

Vol. 18

Firestone, E.R., and S.B. Hooker, 2002: SeaWiFS Postlaunch Technical Report Series Cumulative Index: Volumes 1–17. *NASA Tech. Memo. 2002–206892, Vol. 18,* S.B. Hooker and E.R. Firestone, Eds., NASA Goddard Space Flight Center, Greenbelt, Maryland, (in prep.).

Vol. 19

Zibordi, G., J-F. Berthon, J.P. Doyle, S. Grossi, D. van der Linde, C. Targa, and L. Alberotanza 2002: Coastal Atmosphere and Sea Time Series (CoASTS), Part 1: A Tower-Based Long-Term Measurement Program. *NASA Tech. Memo. 2002–206892, Vol. 19,* S.B. Hooker and E.R. Firestone, Eds., NASA Goddard Space Flight Center, Greenbelt, Maryland, 29 pp.

Vol. 20

Berthon, J-F., G. Zibordi, J.P. Doyle, S. Grossi, D. van der Linde, and C. Targa, 2002: Coastal Atmosphere and Sea Time Series (CoASTS), Part 2: Data Analysis. *NASA Tech. Memo. 2002–206892, Vol. 20,* S.B. Hooker and E.R. Firestone, Eds., NASA Goddard Space Flight Center, Greenbelt, Maryland, 25 pp.

Vol. 21

Zibordi, G., D. D'Alimonte, D. van der Linde, J-F. Berthon, S.B. Hooker, J.L. Mueller, G. Lazin, and S. McLean, 2002: The Eighth SeaWiFS Intercalibration Round-Robin Experiment (SIRREX-8), September–December 2001. *NASA Tech. Memo. 2002–206892, Vol. 21,* S.B. Hooker and E.R. Firestone, Eds., NASA Goddard Space Flight Center, Greenbelt, Maryland, 39 pp.

REPORT DOCUMENTATION PAGE

Form Approved
OMB No. 0704-0188

1. AGENCY USE ONLY *(Leave blank)*	2. REPORT DATE	3. REPORT TYPE AND DATES COVERED
	December 2002	Technical Memorandum

4. TITLE AND SUBTITLE

SeaWiFS Postlaunch Technical Report Series
Volume 21: The Eighth SeaWiFS Intercalibration Round-Robin Experiment (SIRREX-8), September–December 2001

5. FUNDING NUMBERS

970.2

6. AUTHORS

G. Zibordi, D. D'Alimonte, D. van der Linde, J-F. Berthon, S.B. Hooker, J.L. Mueller, G. Lazin, and S. McLean

Series Editors: Stanford B. Hooker and Elaine R. Firestone

7. PERFORMING ORGANIZATION NAME(S) AND ADDRESS(ES)

Laboratory for Hydrospheric Processes
Goddard Space Flight Center
Greenbelt, Maryland 20771

8. PERFORMING ORGANIZATION REPORT NUMBER

2003-00247-1

9. SPONSORING/MONITORING AGENCY NAME(S) AND ADDRESS(ES)

National Aeronautics and Space Administration
Washington, D.C. 20546–0001

10. SPONSORING/MONITORING AGENCY REPORT NUMBER

TM—2002–206892, Vol. 21

11. SUPPLEMENTARY NOTES

E.R. Firestone: Science Applications International Corporation, Beltsville, Maryland; G. Zibordi, D. D'Alimonte, D. van der Linde, and J-F. Berthon: JRC/Institute for Environment and Sustainability, Ispra, Italy; J.L. Mueller: SDSU/Center for Hydro-Optics and Remote Sensing, San Diego, California; and G. Lazin, and S. McLean: Satlantic, Inc., Halifax, Canada

12a. DISTRIBUTION/AVAILABILITY STATEMENT

Unclassified–Unlimited
Subject Category 48
Report is available from the Center for AeroSpace Information (CASI), 7121 Standard Drive, Hanover, MD 21076–1320; (301)621-0390

12b. DISTRIBUTION CODE

13. ABSTRACT *(Maximum 200 words)*

This report documents the scientific activities during the eighth SeaWiFS Intercalibration Round-Robin Experiment (SIRREX-8) held at the Center for Hydro-Optics and Remote Sensing (CHORS), the Joint Research Centre (JRC), and Satlantic, Inc. The objectives of SIRREX-8 were to a) quantify the uncertainties associated with measuring the immersion factor with a standard protocol, b) establish if instrument-to-instrument variability prevents the assignment of a set of immersion factors for an entire series of sensors, c) compare average immersion factors obtained from sample OCI-200 radiometers with those provided by Satlantic for the same series of instruments, and d) measure the cosine response of one sensor at CHORS and Satlantic. An overview of SIRREX-8 is given in Chapt. 1, the immersion factor methods used by the participating laboratories are presented in Chapters 2–4, and the data processing code is documented in Chapt. 5. The cosine response methods and results are presented in Chapt. 6, along with an analysis of the data. A synthesis of the immersion factor results is presented in Chapt. 7 and includes a discussion and conclusion of the effort with respect to the objectives.

14. SUBJECT TERMS

SeaWiFS, Oceanography, SIRREX, Intercalibration, Round-Robin Experiment, Lamps, Plaques, Standards, Uncertainty

15. NUMBER OF PAGES

39

16. PRICE CODE

17. SECURITY CLASSIFICATION OF REPORT	18. SECURITY CLASSIFICATION OF THIS PAGE	19. SECURITY CLASSIFICATION OF ABSTRACT	20. LIMITATION OF ABSTRACT
Unclassified	Unclassified	Unclassified	Unlimited